Ishibashi, Ryuji Kohno	Capability of Low Duty-Cycle UWB Communications in the Presence of Wideband OFDM System	Personal Communicatio ns Journal, Springer	10.1007	9-9713-4	4
Haruka Suzuki, Marco Hernandez, Ryuji Kohno	Hybrid ARQ Error-Controlling Scheme for Robust and Efficient Transmission of a UWB Body Area Network	IEICE on Communicatio ns	Vol. E93 -B, No. 0 4, pp		2010
Hideaki Miura, Ryuji Kohno	Frequency Dependent Dispersion Compensation Method of Electromagnetic Waves Hyperthermia Using Time Reversal Waves	The 6th Conference of Asia Pacific Association for Medical Informatics 2009 (APAMI 2009),		pp. P-65	2009
Hideki Mochizuki, Masayuki Hayashi, Ryuji Kohno	Study on Medical and non-Medical UWBTransmission Schemes in Wearable Body Area Network	The 4th International Symposium on Medical Information and Communicatio n Technology (ISMICT2010)			2010
Haruka Suzuki, Marco Hernandez, Ryuji Kohno	Hybrid ARQ Error-Controlling Scheme for Robust and Efficient Transmission of a UWB Body Area Network	The 4th International Symposium on Medical Information and Communicatio ns Technology (ISMICT 2010)			2010
鈴木晴香，林雅之，河野隆二	医療・非医療用ボディエリアネットワークに適した Hybrid ARQ Type2 誤り制御法	電子情報通信学会ソサイエティ大会	A-5-11		2009
望月英希, 河野隆二	WBAN に適した高信頼度医療用通信方式の研究	電子情報通信学会ソサイエティ大会	A-5-10		2009
三浦英朗、河野隆二	時間反転波による電磁波ハイパーサーミアの減衰補償法の検討	電子情報通信学会ソサイエ	A-5-12		2009

		ティ大会 2009			
望月英希, 林雅之, 河野隆二	WBAN 環境下における医療用・非医療用 Pulsed Chirp UWB 方式の特性評価	第 32 回情報理論とその応用シンポジウム (SITA2009)		pp.787-792	2009
三浦英朗、河野隆二	複数のガンがある場合の時間反転波による電磁波ハイパーサーミアについての検討	第 3 回医療情報通信技術研究会 (MICT)	no.3	pp.19-26	2010
鈴木晴香, Marco Hernandez, 河野隆二	UWB 無線通信を用いたウェアラブルボディエリアネットワークのための Hybrid ARQ による誤り制御に関する検討	電子情報通信学会総合大会			2010
T. Miyake, M. Oike, S. Yoshino, Y. Yatagawa, K. Haneda, H. Kaji, M. Nishizawa	Biofuel cell anode: NAD+/glucose dehydrogenase-coimmobilized ketjenblack electrode	Chem. Phys. Lett	480	123-126	2009
M. Togo, K. Morimoto, H. Kaji, T. Abe, M. Nishizawa	Series-connected biofuel cells in a microfluidic channel with superhydrophobic air valve	Digest of Technical Papers, Transducers09		2102-2105	2009
都甲真, 西澤松彦	酵素燃料電池の新潮流	酵素工学ニュース	59	16−20	2009
三宅丈雄、西澤松彦	バイオ電池の最新開発動向	Semiconductor FPD World	29	48-49	2010

Neurochemistry International xxx (2009) xxx–xxx

Contents lists available at ScienceDirect

Neurochemistry International

journal homepage: www.elsevier.com/locate/neuint

Role of Ca^{2+}-activated K^+ channels in catecholamine release from *in vivo* rat adrenal medulla

Tsuyoshi Akiyama [a,*], Toji Yamazaki [a], Toru Kawada [b], Shuji Shimizu [b], Masaru Sugimachi [b], Mikiyasu Shirai [a]

[a] Department of Cardiac Physiology, National Cardiovascular Center Research Institute, 5-7-1 Fujishiro-dai, Suita, 565-8565 Osaka, Japan
[b] Department of Cardiovascular Dynamics, National Cardiovascular Center Research Institute, Suita, 565-8565, Japan

ARTICLE INFO

Article history:
Received 24 September 2009
Received in revised form 21 October 2009
Accepted 28 October 2009
Available online xxx

Keywords:
Anesthetized rats
Microdialysis technique
Acetylcholine
Norepinephrine
Epinephrine
Ca^{2+}-activated K^+ channels

ABSTRACT

To elucidate the role of Ca^{2+}-activated K^+ (K_{Ca}) channels in the presynaptic acetylcholine (ACh) release from splanchnic nerve endings and the postsynaptic catecholamine release from chromaffin cells, we applied microdialysis technique to the left adrenal medulla of anesthetized rats and investigated the effects of local administration of K_{Ca} channel antagonists through dialysis probes on the release of ACh and/or catecholamine, induced by electrical stimulation of splanchnic nerves or local administration of ACh through the dialysis probes. *Nerve stimulation-induced release*: in the presence of a cholinesterase inhibitor, neostigmine, large-conductance K_{Ca} (BK) channel antagonists, iberiotoxin and paxilline enhanced the presynaptic ACh release and postsynaptic norepinephrine (NE) and epinephrine (Epi) release. Small-conductance K_{Ca} (SK) channel antagonists, apamin and scyllatoxin enhanced the Epi release without any changes in ACh or NE release. In the absence of neostigmine, ACh release was not detected. Iberiotoxin and paxilline enhanced NE and Epi release. Apamin and scyllatoxin had no effect on NE or Epi release. *Exogenous ACh-induced release*: iberiotoxin and paxilline enhanced the Epi release, but had no effect on the NE release. Apamin and scyllatoxin enhanced both NE and Epi release. In conclusion, BK channels on splanchnic nerve endings play an inhibitory role in the physiological catecholamine release from adrenal medulla by limiting presynaptic ACh release while SK channels do not. BK channels on Epi-storing cells may play an inhibitory role in nerve stimulation-induced Epi release. SK channels on NE- and Epi-storing cells play a minor role in nerve stimulation-induced catecholamine release.

1. Introduction

The physiological release of catecholamine from adrenal medulla is controlled by central sympathetic neurons through splanchnic nerves. Splanchnic nerve endings make synaptic-like contacts with chromaffin cells (Coupland, 1965). Activation of splanchnic nerve endings causes Ca^{2+} influx through voltage-dependent Ca^{2+} channels, which evokes exocytotic acetylcholine (ACh) release. This ACh release activates cholinergic receptors on chromaffin cells, which causes Ca^{2+} influx through voltage-dependent Ca^{2+} channels and evokes exocytotic catecholamine release from chromaffin cells (García et al., 2006).

Ca^{2+}-activated K^+ (K_{Ca}) currents are consistently found at neuronal cells or nerve terminals (Meir et al., 1999). K_{Ca} channels are located in the vicinity of voltage-dependent Ca^{2+} channels and activated by Ca^{2+} influx through voltage-dependent Ca^{2+} channels. Activation of the K_{Ca} channels induces outward efflux of K^+, causes hyperpolarization of the membrane, and subsequently limits Ca^{2+} entry through voltage-dependent Ca^{2+}channels. Thus, K_{Ca} channels may be present at two different sites in the adrenal medulla: splanchnic nerve endings and chromaffin cells, and are then involved in the physiological regulation of presynaptic ACh release and/or postsynaptic catecholamine release. In fact, it has been reported that K_{Ca} channels on chromaffin cells play an important role in catecholamine release (Montiel et al., 1995; Uceda et al., 1992; Wada et al., 1995). Little information is, however, available on the role of K_{Ca} channels in the presynaptic ACh release from splanchnic nerve endings.

We have recently developed a dialysis technique to simultaneously monitor the release of presynaptic ACh and postsynaptic catecholamine in the *in vivo* adrenal medulla (Akiyama et al., 2004a). This method makes it possible to investigate the functional roles of K_{Ca} channels in the ACh release from splanchnic nerve endings and the catecholamine release from adrenal medulla in the *in vivo* state. In the present study, we applied the microdialysis technique to the adrenal medulla of anesthetized rats and investigated the effects of K_{Ca} channel antagonists on the release of presynaptic ACh and postsynaptic catecholamine.

* Corresponding author. Tel.: +81 6 6833 5012x2380; fax: +81 6 6872 8092.
E-mail address: takiyama@ri.ncvc.go.jp (T. Akiyama).

0197-0186/$ – see front matter © 2009 Elsevier Ltd. All rights reserved.
doi:10.1016/j.neuint.2009.10.010

In electrophysiological studies, K_{Ca} channels can be divided into two types based on their single channel conductance: large-conductance (BK) and small-conductance K_{Ca} (SK) channels (Blatz and Magleby, 1987). We tested two types of BK channel antagonists: the selective peptidergic BK channel antagonist, iberiotoxin (Candia et al., 1992) and the non-peptidergic BK channel antagonist, paxilline (Kanus et al., 1994). Similarly we tested two types of SK channel antagonists: the selective peptidergic SK channel antagonist, apamin (Blatz and Magleby, 1986) and the selective peptidergic SK channel antagonist different in amino acid sequence, scyllatoxin (Auguste et al., 1990).

2. Materials and methods

2.1. Animal preparation

Animal care was provided in strict accordance with the *Guiding Principles for the Care and Use of Animals in the Field of Physiological Sciences* approved by the Physiological Society of Japan. All protocols were approved by the Animal Subject Committee of the National Cardiovascular Center. Adult male Wistar rats weighing 380–460 g were anesthetized with pentobarbital sodium (50–55 mg/kg, i.p.). A cervical midline incision was made to expose the trachea, which was then cannulated. The rats were ventilated with a constant-volume respirator using room air mixed with oxygen. The left femoral artery and vein were cannulated for monitoring arterial blood pressure and administration of anesthetic, respectively. The level of anesthesia was maintained with a continuous intravenous infusion of pentobarbital sodium (15–25 mg/kg/h, i.v.). The electrocardiogram was monitored to record the heart rate. A thermostatic heating pad was used to keep the esophageal temperature within a range of 37–38 °C. With the animal in the lateral position, the left adrenal gland and left splanchnic nerve were exposed by a subcostal flank incision, and the left splanchnic nerve was transected. In protocols requiring nerve stimulation, shielded bipolar stainless steel electrodes were applied to the distal end of the nerve, which was then stimulated with a digital stimulator (SEN-7203, Nihon Kohden, Japan) with a rectangular pulse (10 V and 1 ms in duration).

2.2. Dialysis technique

Dialysis probe construction was the same as that used in our previous dialysis experiments (Akiyama et al., 2003, 2004a,b). Each end of a dialysis fiber (0.32 mm OD, and 0.25 mm ID; PAN-DX 100,000 mol wt 100% cutoff, Asahi Chemical, Japan) was inserted into a polyethylene tube (25 cm length, 0.5 mm OD, and 0.2 mm ID; SP-8) and glued. The length of the dialysis fiber exposed was 3 mm. At a perfusion speed of 10 μl/min, *in vitro* recovery rates of ACh, norepinephrine (NE) and epinephrine (Epi) were (%): 3.21 ± 0.07, 2.68 ± 0.03, and 2.80 ± 0.03, respectively (number of dialysis probes: 3).

The left adrenal gland was gently lifted, and the dialysis probe was implanted in the medulla of the left adrenal gland along the long axis using a fine guiding needle. The dialysis probe was perfused with Ringer's solution or Ringer's solution containing pharmacological agents at a speed of 10 μl/min using a microinjection pump (CMA/100, Carnegie Medicin, Sweden). Ringer's solution consisted of (in mM) 147.0 NaCl, 4.0 KCl, 2.25 $CaCl_2$. All K_{Ca} channel antagonists tested were locally administered by perfusion through the dialysis probe after being dissolved in Ringer's solution. We started the protocols followed by a stabilization period of 3–4 h and sampled dialysate taking the dead space volume between the dialysis membrane and sample tube into account. Dialysate ACh and catecholamine concentrations were separately measured using each high-performance liquid chromatography with electrochemical detection as previously described (Akiyama et al., 2004a,b).

2.3. Experimental protocols

The experiment was performed based on the previous experiment showing that dialysate ACh and/or catecholamine responses were reproducible on repetition of the pharmacological or electrical stimulation (Akiyama et al., 2004a,b). At the end of the experiment, the rats were sacrificed with pentobarbital sodium, and the implant sites were examined. The dialysis probes were confirmed to have been implanted in the adrenal medulla, and no bleeding or necrosis was found macroscopically.

2.4. Protocol 1

We perfused the dialysis probe with Ringer's solution containing a cholinesterase inhibitor, neostigmine (10 μM) and investigated the effects of BK and SK channel antagonists on the nerve stimulation-induced responses of dialysate ACh and catecholamine concentration. The left splanchnic nerves were firstly electrically stimulated for 2 min at 2 Hz. Then, after a 30-min interval, nerves were subjected to a second stimulation for 2 min at 4 Hz. After these control stimulations, local administration of iberiotoxin (1 μM, $n = 7$), paxilline (100 μM, $n = 7$), apamin (10 μM, $n = 7$) or scyllatoxin (2 μM, $n = 7$) was started. Thirty minutes after local administration of K_{Ca} channel antagonists, nerves were stimulated for 2 min at 2 Hz. Next, after a 30-min interval, nerves were stimulated again for 2 min at 4 Hz. Phosphate buffer (pH 3.5, 4 μl) was transferred into each sample tube before dialysate sampling. Two dialysate samples were continuously collected per nerve stimulation: one before and one during stimulation. One sampling period was 2 min (1 sample volume = 20 μl). Half of the dialysate sample was used for the measurement of ACh, and the remaining half for the measurement of NE and Epi.

2.5. Protocol 2

We investigated the effects of K_{Ca} channel antagonists on the nerve stimulation-induced catecholamine release in the absence of neostigmine. Like in protocol 1, the left splanchnic nerves were stimulated before and 30 min after administration of iberiotoxin ($n = 7$), paxilline ($n = 7$), apamin ($n = 7$) or scyllatoxin ($n = 7$) and two dialysate samples were collected per nerve stimulation. The dialysate sample was used for the measurement of NE and Epi.

2.6. Protocol 3

We investigated the effects of K_{Ca} channel antagonists on exogenous ACh-induced catecholamine release. The dialysis probe was perfused with Ringer's solution. ACh (1 mM) was locally administered to the adrenal medulla through the dialysis probe for 1 min. After first administration of ACh, local administration of iberiotoxin (1 μM, $n = 7$), paxilline (100 μM, $n = 7$), apamin (10 μM, $n = 7$) or scyllatoxin (2 μM, $n = 7$) was started. Thirty minutes after local administration of K_{Ca} channel antagonists, ACh (1 mM) was locally administered again for 1 min. Phosphate buffer (pH 3.5, 2 μl) was transferred into each sample tube before dialysate sampling. Two dialysate samples were continuously collected per local administration of ACh: one before and one during administration. One sampling period was 1 min (1 sample volume = 10 μl). The dialysate sample was used for the measurement of NE and Epi.

2.7. Drugs

Drugs were mixed fresh for each experiment. Neostigmine methylsulfate (Shionogi, Japan), iberiotoxin (Peptide Institute, Japan), apamin (Peptide Institute) and scyllatoxin (Peptide Institute) were dissolved and diluted in Ringer's solution. Paxilline (Sigma Chemical, USA) was dissolved in DMSO and diluted in Ringer's solution. The final concentration of DMSO in the working solution was 0.5% (v/v).

2.8. Statistical methods

To examine the effects of nerve stimulation, local administration of ACh, and K_{Ca} channel antagonists, we analyzed heart rate and mean arterial pressure, basal dialysate NE and Epi content, and dialysate ACh, NE and Epi responses, by using one-way analysis of variance with repeated measures. When statistical significance was detected, the Newman–Keuls test was applied (Winer, 1971). Statistical significance was defined as $P < 0.05$. Values are presented as means ± SE.

3. Results

3.1. Changes in heart rate and mean arterial pressure

Local administration of neostigmine, K_{Ca} channel antagonists, and ACh through the dialysis probe did not change basal heart rate or mean arterial pressure. In protocol 1, nerve stimulation increased mean arterial pressure from 113 ± 3 mmHg in control to 131 ± 2 mmHg at 2 Hz ($n = 28$, $P < 0.05$) and 132 ± 2 mmHg at 4 Hz ($n = 28$, $P < 0.05$), and decreased heart rate from 436 ± 4 beats/min in control to 424 ± 4 beats/min at 2 Hz ($n = 28$, $P < 0.05$) and 420 ± 4 beats/min at 4 Hz ($n = 28$, $P < 0.05$). In protocol 2, nerve stimulation increased mean arterial pressure from 115 ± 4 mmHg in control to 129 ± 3 mmHg at 2 Hz ($n = 28$, $P < 0.05$) and 131 ± 3 mmHg at 4 Hz ($n = 28$, $P < 0.05$), and decreased heart rate from 423 ± 3 beats/min in control to 410 ± 4 beats/min at 2 Hz ($n = 28$, $P < 0.05$) and 404 ± 3 beats/min at 4 Hz ($n = 28$, $P < 0.05$). Heart rate and mean arterial pressure recovered to basal levels after nerve stimulation. After administration of K_{Ca} channel antagonists, nerve stimulation evoked the same responses of heart rate and mean arterial pressure.

Please cite this article in press as: Akiyama, T., et al., Role of Ca^{2+}-activated K^+ channels in catecholamine release from *in vivo* rat adrenal medulla. Neurochem. Int. (2009), doi:10.1016/j.neuint.2009.10.010

Table 1
Basal NE and Epi release before and after local administration of K_{Ca} channel antagonists.

	NE (nM)	Epi (nM)
Iberiotoxin ($n=21$)		
Before administration	4.8 ± 0.3	16.7 ± 1.0
After administration	5.0 ± 0.4	21.7 ± 1.6*
Paxilline ($n=21$)		
Before administration	4.7 ± 0.3	15.7 ± 1.1
After administration	4.8 ± 0.4	22.0 ± 1.9*
Apamin ($n=21$)		
Before administration	4.9 ± 0.4	17.1 ± 1.1
After administration	4.6 ± 0.5	21.2 ± 1.6*
Scyllatoxin ($n=21$)		
Before administration	4.9 ± 0.3	15.3 ± 0.7
After administration	5.1 ± 0.4	20.6 ± 0.9*

Values are means ± SE. *n*, no. of rats; NE, norepinephrine; Epi, epinephrine. *$P < 0.05$ vs. values before administration.

3.2. Basal ACh and catecholamine release

ACh could not be detected in dialysate before nerve stimulation even in the presence of neostigmine. In contrast, substantial amounts of NE and Epi were observed in dialysate before nerve stimulation or ACh administration. Local administration of neostigmine did not influence this basal catecholamine release. BK channel antagonists, iberiotoxin and paxilline did not change basal NE release but increased basal Epi release. Similarly, the SK channel antagonists, apamin and scyllatoxin did not change basal NE release, but increased basal Epi release (Table 1).

ACh was detected in dialysate only during nerve stimulation in the presence of neostigmine. Thus, we expressed this detected dialysate ACh concentration as an index of ACh release induced by nerve stimulation. In contrast, we subtracted basal dialysate NE and Epi content before nerve stimulation or ACh administration from those during stimulation or ACh administration, and expressed these subtracted values as indices of NE and Epi release induced by nerve stimulation or ACh administration.

3.3. Effects of K_{Ca} channel antagonists on the nerve stimulation-induced ACh and catecholamine release in the presence of neostigmine

Iberiotoxin enhanced the nerve stimulation-induced release of presynaptic ACh and postsynaptic catecholamine (Fig. 1A). ACh release increased from 4.5 ± 0.8 to 7.4 ± 0.7 nM at 2 Hz and from 9.4 ± 1.0 to 14.0 ± 1.0 nM at 4 Hz. NE release increased from 7 ± 0.5 to 32 ± 3 nM at 2 Hz and from 27 ± 3 to 74 ± 9 nM at 4 Hz. Epi release increased from 39 ± 5 to 78 ± 5 nM at 2 Hz, and from 105 ± 8 to 193 ± 15 nM at 4 Hz. Similarly, paxilline enhanced the nerve stimulation-induced release of ACh and catecholamine (Fig. 1B). ACh release increased from 4.1 ± 0.4 to 5.9 ± 0.5 nM at 2 Hz and from 9.4 ± 0.7 to 13.7 ± 0.9 nM at 4 Hz. NE release increased from 11 ± 2 to 26 ± 4 nM at 2 Hz, from 31 ± 5 to 58 ± 8 nM at 4 Hz. Epi release increased from 41 ± 7 to 77 ± 14 nM at 2 Hz and from 108 ± 14 to 195 ± 17 nM at 4 Hz.

Apamin had no effect on the nerve stimulation-induced release of ACh and NE, but enhanced the nerve stimulation-induced Epi release (Fig. 2A). Epi release increased from 45 ± 3 to 59 ± 4 nM at 2 Hz and from 108 ± 7 to 139 ± 17 nM at 4 Hz. Scyllatoxin had no effect on the nerve stimulation-induced release of ACh and NE either, but enhanced the nerve stimulation-induced Epi release (Fig. 2B). Epi release increased from 37 ± 4 to 50 ± 3 nM at 2 Hz and from 122 ± 5 to 152 ± 12 nM at 4 Hz.

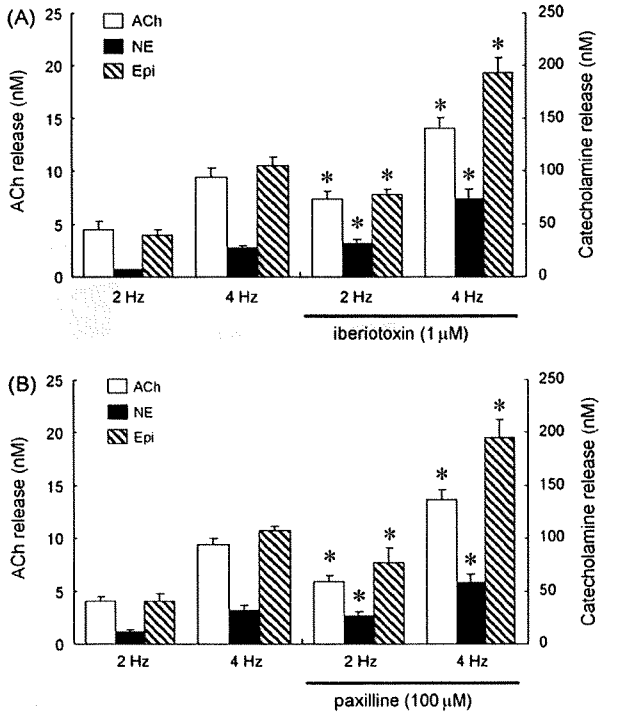

Fig. 1. Effects of BK channel antagonists on the nerve stimulation-induced release of acetylcholine (ACh), norepinephrine (NE) and epinephrine (Epi) in the presence of neostigmine (10 μM): iberiotoxin (A) and paxilline (B) enhanced the release of ACh, NE and Epi at 2 and 4 Hz. Values are means ± SE from seven rats. *$P < 0.05$ vs. ACh, NE or Epi release at the same frequency as before administration of BK channel antagonists.

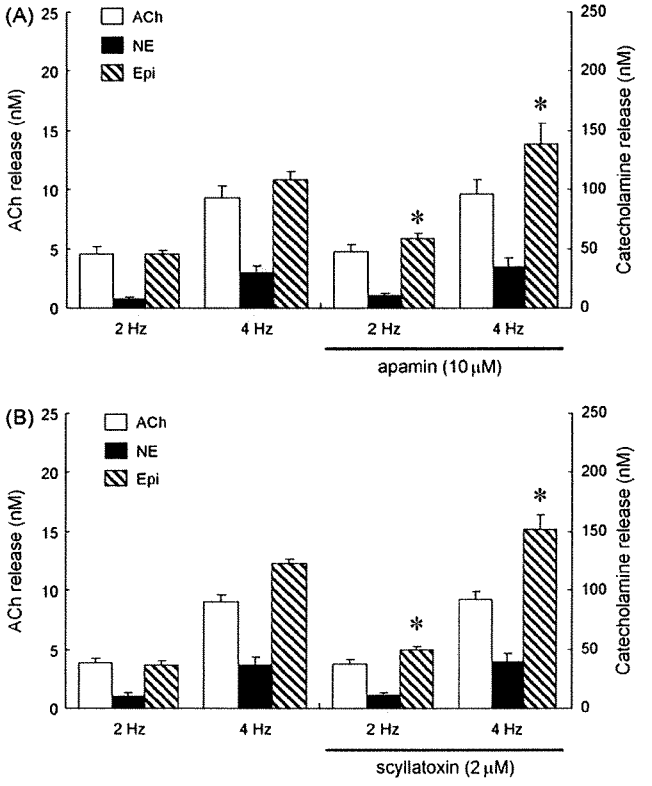

Fig. 2. Effects of SK channel antagonists on the nerve stimulation-induced release of ACh, NE and Epi in the presence of neostigmine (10 μM): apamin (A) and scyllatoxin (B) had no effect on the release of ACh or NE, but enhanced the Epi release at 2 and 4 Hz. Values are means ± SE from seven rats. *$P < 0.05$ vs. ACh, NE or Epi release at the same frequency as before administration of SK channel antagonists.

Please cite this article in press as: Akiyama, T., et al., Role of Ca^{2+}-activated K^+ channels in catecholamine release from *in vivo* rat adrenal medulla. Neurochem. Int. (2009), doi:10.1016/j.neuint.2009.10.010

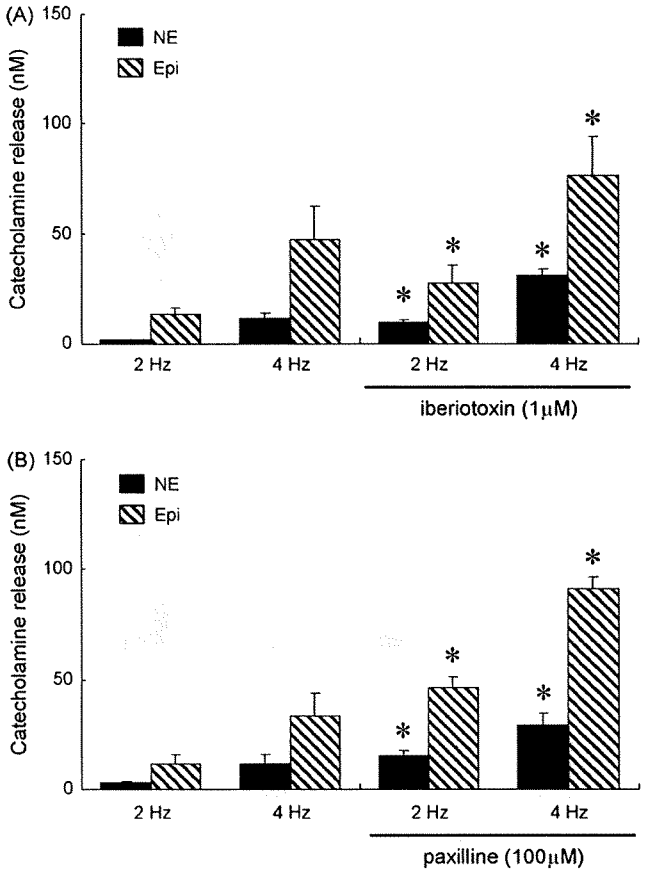

Fig. 3. Effects of BK channel antagonists on the nerve stimulation-induced release of NE and Epi in the absence of neostigmine: iberiotoxin (A) and paxilline (B) enhanced the release of NE and Epi at 2 and 4 Hz. Values are means ± SE from seven rats. *$P < 0.05$ vs. NE or Epi release at the same frequency as before administration of BK channel antagonists.

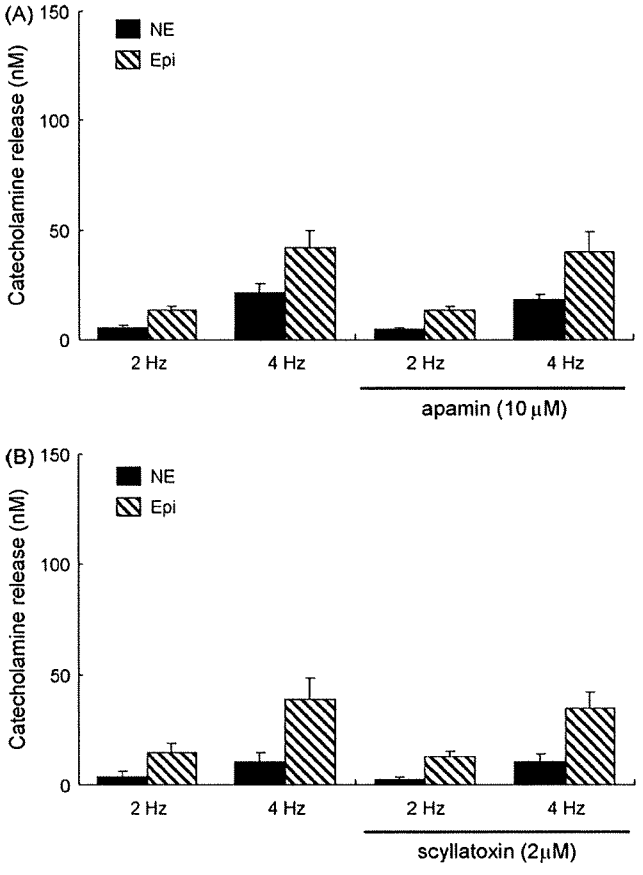

Fig. 4. Effects of SK channel antagonists on the nerve stimulation-induced release of NE and Epi in the absence of neostigmine: apamin (A) and scyllatoxin (B) had no effect on the release of NE or Epi at 2 or 4 Hz. Values are means ± SE from seven rats.

3.4. Effects of K_{Ca} channel antagonists on the nerve stimulation-induced catecholamine release in the absence of neostigmine

Iberiotoxin enhanced the nerve stimulation-induced catecholamine release at both 2 and 4 Hz (Fig. 3A). NE release increased from 2 ± 0.3 to 10 ± 2 nM at 2 Hz and from 12 ± 3 to 31 ± 3 nM at 4 Hz. Epi release increased from 13 ± 3 to 27 ± 9 nM at 2 Hz and from 47 ± 15 to 76 ± 18 nM at 4 Hz. Similarly, paxilline enhanced the nerve stimulation-induced catecholamine release (Fig. 3B). NE release increased from 3 ± 0.6 to 15 ± 2 nM at 2 Hz and from 12 ± 4 to 29 ± 5 nM at 4 Hz. Epi release increased from 12 ± 4 to 46 ± 5 nM at 2 Hz and from 34 ± 10 to 91 ± 6 nM at 4 Hz. Apamin and scyllatoxin had no effect on the nerve stimulation-induced catecholamine release at 2 or 4 Hz (Fig. 4A and B).

3.5. Effects of K_{Ca} channel antagonists on the exogenous ACh-induced catecholamine release

Iberiotoxin had no effect on the exogenous ACh-induced NE release, but enhanced the exogenous ACh-induced Epi release. Epi release increased from 108 ± 11 to 127 ± 10 nM (Fig. 5A). Similarly, paxilline had no effect on the exogenous ACh-induced NE release but enhanced the exogenous ACh-induced Epi release. Epi release increased from 93 ± 5 to 137 ± 13 nM (Fig. 5B). Apamin enhanced the exogenous ACh-induced catecholamine release (Fig. 6A). NE release increased from 37 ± 4 to 49 ± 4 nM and Epi release from 103 ± 8 to 122 ± 9 nM. Similarly scyllatoxin enhanced the exogenous ACh-induced catecholamine release (Fig. 6B). NE release increased from 32 ± 3 to 47 ± 3 nM and Epi release from 108 ± 6 to 140 ± 11 nM.

4. Discussion

4.1. Roles of K_{Ca} channels on splanchnic nerve endings in presynaptic ACh release

We found that, in the *in vivo* adrenal medulla, both iberiotoxin and paxilline enhanced the nerve stimulation-induced release of presynaptic ACh at 2 and 4 Hz by ~50% in the presence of neostigmine (Fig. 1). BK channels currents have been confirmed on cholinergic nerve endings including motor nerves in the neuromuscular junction (Flink and Atchison, 2003), presynaptic nerves in the chick ciliary ganglion (Sun et al., 1999) and tracheal parasympathetic nerves (Zhang et al., 1998). Activation of the K_{Ca} conductance is considered to limit Ca^{2+} entry through voltage-dependent Ca^{2+}channels, and subsequently reduce transmitter release (Meir et al., 1999). Our results strongly suggest that BK channels are present on the splanchnic nerve endings and involved in the control of ACh release. In the perfused cat adrenal gland, charybdotoxin, a BK channel antagonist, enhanced catecholamine release when transmural electrical stimulation was applied at low external Ca^{2+} concentrations, but not when exogenous ACh was administered (Montiel et al., 1995). In the perfused rat adrenal gland, charybdotoxin enhanced the release of Epi and NE induced by transmural electrical stimulation, but not the release induced by administration of ACh (Nagayama et al., 2000b). These indirect studies suggested that BK channels may be involved in the control

Please cite this article in press as: Akiyama, T., et al., Role of Ca^{2+}-activated K^+ channels in catecholamine release from *in vivo* rat adrenal medulla. Neurochem. Int. (2009), doi:10.1016/j.neuint.2009.10.010

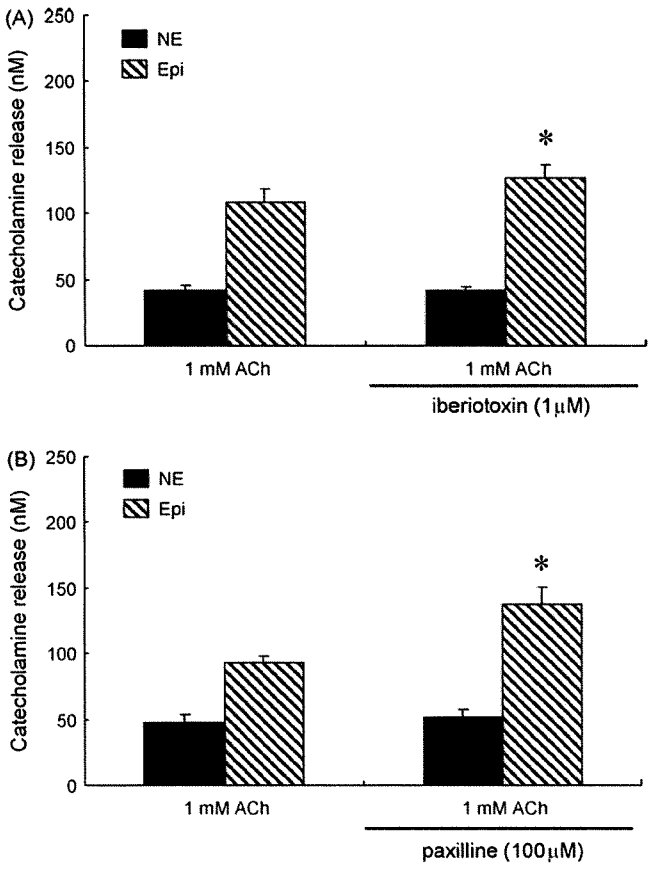

Fig. 5. Effects of BK channel antagonists on the exogenous ACh-induced release of NE and Epi: iberiotoxin (A) and paxilline (B) had no effect on NE release, but enhanced Epi release. Values are means ± SE from seven rats. $^*P < 0.05$ vs. NE or Epi release before administration of BK channel antagonists.

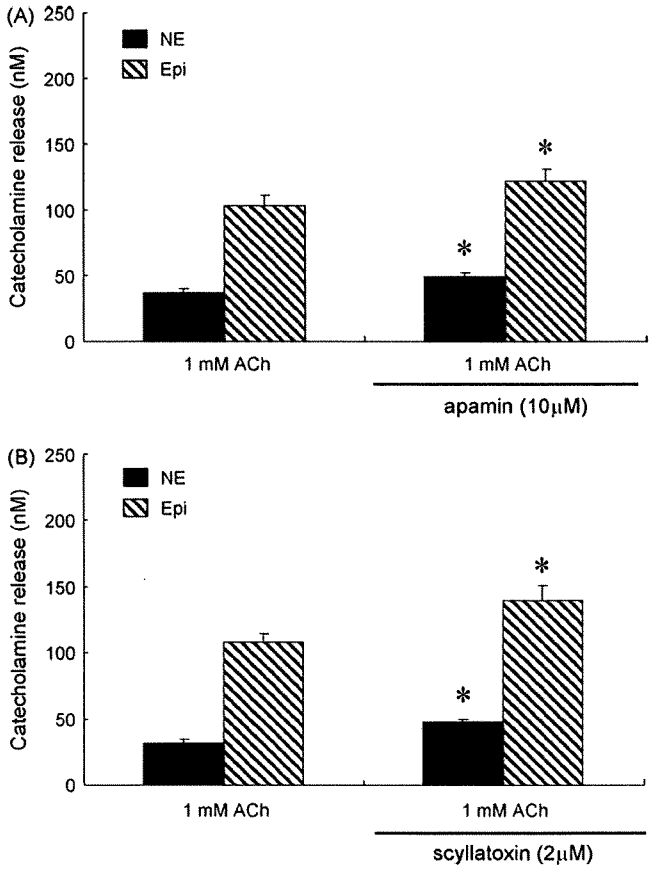

Fig. 6. Effects of SK channel antagonists on the exogenous ACh-induced release of NE and Epi: apamin (A) and scyllatoxin (B) enhanced the release of NE and Epi. Values are means ± SE from seven rats. $^*P < 0.05$ vs. NE or Epi release before administration of SK channel antagonists.

of catecholamine release at the presynaptic site. But there has been no direct study investigating the effect of BK channel antagonists on ACh release from splanchnic nerve endings. This is the first direct study to demonstrate that BK channels are involved in the control of ACh release from splanchnic nerve endings. In the *in vivo* adrenal medulla, we observed a substantial enhancement of ACh release by BK channel antagonists at a frequency of 2 Hz with this degree of enhancement being similar to that at a frequency of 4 Hz (Fig. 1). BK channels on splanchnic nerve endings could be functional under physiological conditions. In our previous study, the nerve stimulation-induced catecholamine release was in large part cholinergic in the presence or absence of neostigmine (Akiyama et al., 2003). Thus, BK channels play an inhibitory role in the physiological catecholamine release from adrenal medulla by limiting presynaptic ACh release.

In contrast to BK channel antagonists, apamin and scyllatoxin had no effect on the nerve stimulation-induced ACh release at 2 or 4 Hz (Fig. 2). In perfused cat adrenal glands preloaded with [^{3}H]-choline, apamin did not modify the efflux of [^{3}H]-labeled compound evoked by transmural electrical stimulation (Montiel et al., 1995). SK channels seem to be absent on splanchnic nerve endings or play a minor role in the ACh release from splanchnic nerve endings.

4.2. Role of K_{Ca} channels on chromaffin cells in catecholamine release

Iberiotoxin and paxilline had no effect on the exogenous ACh-induced NE release, but enhanced exogenous ACh-induced Epi release (Fig. 5). Adrenal chromaffin cells are divided into two populations: NE- and Epi-storing cells (Coupland, 1984). While BK channels seem to be absent on NE-storing cells or play a minor role in the nerve stimulation-induced NE release, BK channels seem to be present on Epi-storing cells. It has been reported that BK channels present at rat chromaffin cells are activated by Ca^{2+} influx and contribute to the rapid termination of action potentials (Prakriya and Lingle, 1999), while iberiotoxin augments the nicotinic receptor-mediated catecholamine secretion from bovine adrenal chromaffin cells (Wada et al., 1995). The enhancement by BK channel antagonists of nerve stimulation-induced Epi release may be in part ascribed to their direct effects on Epi-storing cells. BK channels on Epi-storing cells may be involved in the control of nerve stimulation-induced Epi release. In perfused rat and cat adrenal glands, charybdotoxin, a BK channel antagonist, does not affect the exogenous ACh-induced catecholamine release (Montiel et al., 1995; Nagayama et al., 2000b). Our results of Epi release were inconsistent with these studies, possibly due to differences in the BK channel antagonists used and/or in methodology because charybdotoxin is pharmacologically less selective than iberiotoxin for BK channels (Garcia et al., 1991).

Both apamin and scyllatoxin enhanced the nerve stimulation-induced Epi release in the presence of neostigmine without changes in ACh release (Fig. 2), and the exogenous ACh-induced release of NE and Epi (Fig. 6). These results suggest that SK channels are present on both NE- and Epi-storing cells and that such enhancement is due to the direct effects of SK channel antagonists on chromaffin cells. Neither apamin nor scyllatoxin, however, had any effect on the nerve stimulation-induced NE release in the presence or absence of neostigmine, and the nerve

Please cite this article in press as: Akiyama, T., et al., Role of Ca^{2+}-activated K^+ channels in catecholamine release from *in vivo* rat adrenal medulla. Neurochem. Int. (2009), doi:10.1016/j.neuint.2009.10.010

stimulation-induced Epi release in the absence of neostigmine (Figs. 2 and 4). SK channels on chromaffin cells may play a minor role in the nerve stimulation-induced catecholamine release. It has been reported that SK channels on chromaffin cells are activated by muscarinic receptor stimulation (Nagayama et al., 2000a; Uceda et al., 1992). In our previous study of the same preparation, we demonstrated that muscarinic receptors are present on NE- and Epi-storing cells but play a minor role in the nerve stimulation-induced release of NE and Epi, and that cholinesterase inhibitor elicited muscarinic receptor-mediated Epi release when splanchnic nerve was stimulated (Akiyama et al., 2003). Therefore, SK channels on NE- and Epi-storing cells play an important role in the catecholamine release induced by activation of muscarinic or non-cholinergic receptors including PACAP receptor (Fukushima et al., 2002).

In the perfused rat adrenal gland, apamin enhanced NE release induced by transmural electrical stimulation and a nicotinic receptor agonist (Nagayama et al., 2000b). Therefore, SK channels on NE-storing cells could be activated by nicotinic as well as muscarinic receptors. But, our results of NE release induced by nerve stimulation were inconsistent with this study. In anesthetized dogs, scyllatoxin enhanced catecholamine release induced by a nicotinic receptor agonist but did not affect catecholamine release induced by splanchnic nerve stimulation (Nagayama et al., 1998). Thus, this inconsistency may be due to the difference in the method of nerve stimulation and SK channels on NE-storing cells may be activated by nicotinic receptors in the extrasynaptic region.

4.3. Roles of K_{Ca} channels in basal NE and Epi release

In the present study, substantial basal release of NE and Epi was observed in dialysate before nerve stimulation or ACh administration. Both BK and SK channel antagonists enhanced the basal Epi release but not the basal NE release. In our preparation, splanchnic nerves had been transected before control sampling and basal catecholamine release was not enhanced by a cholinesterase inhibitor, neostigmine. Furthermore, using the same preparation we demonstrated that basal catecholamine release is resistant to not only cholinergic antagonists, but also N-, P/Q-, and L-type Ca^{2+} channel antagonists (Akiyama et al., 2004b). Basal catecholamine release seems to be non-cholinergic and independent of Ca^{2+} influx through voltage-dependent Ca^{2+} channels. Ca^{2+} release from intracellular Ca^{2+} stores may be involved in this basal catecholamine release. It has been suggested in chromaffin cells that K_{Ca} channels on the cell surface are activated by Ca^{2+} release from intracellular Ca^{2+} stores (Ohta et al., 1998). On Epi-storing cells, BK and SK channels may play a role in the Epi release induced by Ca^{2+} release from intracellular Ca^{2+} stores.

4.4. Methodological considerations

Because previous results suggested that distribution across the dialysis membrane is required (Akiyama et al., 2003, 2004a), we used the K_{Ca} channel antagonists at a concentration 10 times higher than that required for complete channel blockade in experimental settings *in vitro*. Then, we tested two different types of selective BK and SK channel antagonists in the present study because higher concentrations of K_{Ca} channel antagonists might induce other pharmacological effects.

Cholinesterase inhibitor was necessary to monitor endogenous ACh even during the splanchnic nerve stimulation because released ACh is rapidly degraded by acetylcholinesterase before reaching the dialysis fiber. Then, we examined the effects of K_{Ca} channel antagonists in the presence or absence of neostigmine because neostigmine may influence the effects of K_{Ca} channel antagonists. Local administration of neostigmine enhanced the nerve stimulation-induced catecholamine release to about 2-fold before and after administration of K_{Ca} channel antagonists (Figs. 1 and 3). This enhancement could be due to the elevation of synaptic ACh levels by inhibition of acetylcholinesterase.

5. Conclusion

We applied dialysis technique to the adrenal medulla of anesthetized rats and investigated the effects of K_{Ca} channel antagonists on the presynaptic ACh release from splanchnic nerve endings and the postsynaptic catecholamine release from chromaffin cells. BK channels on presynaptic splanchnic nerve endings play an inhibitory role in the physiological catecholamine release from adrenal medulla by limiting presynaptic ACh release while SK channels do not. BK channels on Epi-storing cells may play an inhibitory role in the nerve stimulation-induced Epi release. SK channels are present on NE- and Epi-storing cells, but play a minor role in the nerve stimulation-induced catecholamine release.

Acknowledgment

This work was supported by a Grant-in-Aid for scientific research (No. 19591829) from the Ministry of Education, Culture, Sports, Science and Technology.

References

Akiyama, T., Yamazaki, T., Mori, H., Sunagawa, K., 2003. Inhibition of cholinesterase elicits muscarinic receptor-mediated synaptic transmission in the rat adrenal medulla. Auton. Neurosci. 107, 65–73.
Akiyama, T., Yamazaki, T., Mori, H., Sunagawa, K., 2004a. Simultaneous monitoring of acetylcholine and catecholamine release in the in vivo rat adrenal medulla. Neurochem. Int. 44, 497–503.
Akiyama, T., Yamazaki, T., Mori, H., Sunagawa, K., 2004b. Effects of Ca^{2+} channel antagonists on acetylcholine and catecholamine releases in the in vivo rat adrenal medulla. Am. J. Physiol. 287, R161–R166.
Auguste, P., Hugues, M., Gravé, B., Gesquière, J.C., Maes, P., Tartar, A., Romey, G., Schweitz, H., Lazdunski, M., 1990. Leiurotoxin I (scyllatoxin), a peptide ligand for Ca^{2+}-activated K^+ channels. J. Biol. Chem. 265, 4753–4759.
Blatz, A., Magleby, K.L., 1986. Single apamin-blocked Ca-activated K^+ channels of small conductance in cultured rat skeletal muscle. Nature 323, 718–720.
Blatz, A., Magleby, K.L., 1987. Calcium-activated potassium channels. Trends. Neurosci. 10, 463–467.
Candia, S., Garcia, M.L., Latorre, R., 1992. Mode of action of iberiotoxin, a potent blocker of the large conductance Ca^{2+}-activated K^+ channel. Biophys. J. 63, 583–590.
Coupland, R.E., 1965. The Natural History of the Chromaffin Cell. Longmans, London.
Coupland, R.E., 1984. Ultrastructural features of the mammalian adrenal medulla. In: Motta, P.M. (Ed.), Ultrastructure of Endocrine Cells and Tissues. Nijhoff, Boston, MA, pp. 168–179.
Flink, M.T., Atchison, W.D., 2003. Iberiotoxin-induced block of Ca^{2+}-activated K^+ channels induces dihydropyridine sensitivity of ACh release from mammalian motor nerve terminals. J. Pharmacol. Exp. Ther. 305, 646–652.
Fukushima, Y., Nagayama, T., Hikichi, H., Mizukami, K., Yoshida, M., Suzuki-Kusaba, M., Hisa, H., Kimura, T., Satoh, S., 2002. Role of K^+ channels in the PACAP-induced catecholamine secretion from the rat adrenal gland. Eur. J. Pharmacol. 437, 69–72.
García, A.G., García-De-Diego, A.M., Gandía, L., Borges, R., García-Sancho, J., 2006. Calcium signaling and exocytosis in adrenal chromaffin cells. Physiol. Rev. 86, 1093–1131.
Garcia, M.L., Galvez, A., Garcia-Calvo, M., King, V.F., Vazquez, J., Kaczorowski, G.J., 1991. Use of toxins to study potassium channels. J. Bioenerg. Biomembr. 23, 615–646.
Kanus, H.G., McManus, O.B., Lee, S.H., Schmalhofer, W.A., Galcia-Calvo, M., Helms, L.M., Sanchez, M., Giangiacomo, K., Reuben, J.P., Smith, A.B., 1994. Tremorgenic indole alkaloids potently inhibit smooth muscle high-conductance calcium-activated potassium channels. Biochemistry 33, 5819–5828.
Meir, A., Ginsburg, S., Butkevich, A., Kachalsky, S.G., Kaiserman, I., Ahdut, R., Demirgoren, S., Rahamimoff, R., 1999. Ion channels in presynaptic nerve terminals and control of transmitter release. Physiol. Rev. 79, 1019–1088.
Montiel, C., López, M.G., Sánchez-García, P., Maroto, R., Zapater, P., García, A.G., 1995. Contribution of SK and BK channels in the control of catecholamine release by electrical stimulation of the cat adrenal gland. J. Physiol. 486, 427–437.

Please cite this article in press as: Akiyama, T., et al., Role of Ca^{2+}-activated K^+ channels in catecholamine release from *in vivo* rat adrenal medulla. Neurochem. Int. (2009), doi:10.1016/j.neuint.2009.10.010

Nagayama, T., Fukushima, Y., Hikichi, H., Yoshida, M., Suzuki-Kusaba, M., Hisa, H., Kimura, T., Satoh, S., 2000a. Interaction of SK_{Ca} channels and L-type Ca^{2+} channels in catecholamine secretion in the rat adrenal gland. Am. J. Physiol. 279, R1731–R1736.

Nagayama, T., Fukushima, Y., Yoshida, M., Suzuki-Kusaba, M., Hisa, H., Kimura, T., Satoh, S., 2000b. Role of potassium channels in catecholamine secretion in the rat adrenal gland. Am. J. Physiol. 279, R448–R454.

Nagayama, T., Masada, K., Yoshida, M., Suzuki-Kusaba, M., Hisa, H., Kimura, T., Satoh, S., 1998. Role of K^+ channels in adrenal catecholamine secretion in anesthetized dogs. Am. J. Physiol. 274, R1125–R1130.

Ohta, T., Ito, S., Nakazato, Y., 1998. Ca^{2+}-dependent K^+ currents induced by muscarinic receptor activation in guinea pig adrenal chromaffin cells. J. Neurochem. 70, 1280–1288.

Prakriya, M., Lingle, C.J., 1999. BK channel activation by brief deporalizations requires Ca^{2+} influx through L- and Q-type Ca^{2+} channels in rat chromaffin cells. J. Neurophysiol. 81, 2267–2278.

Sun, X.P., Schlichter, L.C., Stanley, E.F., 1999. Single-channel properties of BK-type calcium-activated potassium channels at a cholinergic presynaptic nerve terminal. J. Physiol. 518, 639–651.

Uceda, G., Artalejo, A.R., López, M.G., Abad, F., Neher, E., García, A.G., 1992. Ca^{2+}-activated K^+ channels modulate muscarinic secretion in cat chromaffin cells. J. Physiol. 454, 213–230.

Wada, A., Urabe, M., Yuhi, T., Yamamoto, R., Yanagita, T., Niina, H., Kobayashi, H., 1995. Large- and small-conductance Ca^{2+}-activated K^+ channels: their role in the nicotinic receptor-mediated catecholamine secretion in bovine adrenal medulla. Naunyn Schmiedeberg's Arch. Pharmacol. 352, 545–549.

Winer, B.J., 1971. Statistical Principles in Experimental Design, 2nd ed. McGraw-Hill, New York.

Zhang, X.Y., Zhu, F.X., Robinson, N.E., 1998. Role of cAMP and neuronal K^+ channels on α_2-AR-induced inhibition of ACh release in equine trachea. Am. J. Physiol. 274, L827–L832.

Please cite this article in press as: Akiyama, T., et al., Role of Ca^{2+}-activated K^+ channels in catecholamine release from *in vivo* rat adrenal medulla. Neurochem. Int. (2009), doi:10.1016/j.neuint.2009.10.010

Am J Physiol Heart Circ Physiol 297: H53–H58, 2009.
First published May 15, 2009; doi:10.1152/ajpheart.00260.2009.

Slow head-up tilt causes lower activation of muscle sympathetic nerve activity: loading speed dependence of orthostatic sympathetic activation in humans

Atsunori Kamiya,[1,2] Toru Kawada,[1] Shuji Shimizu,[1] Satoshi Iwase,[2,3] Masaru Sugimachi,[1] and Tadaaki Mano[2,4]

[1]*Department of Cardiovascular Dynamics, National Cardiovascular Center Research Institute, Suita;* [2]*Research Institute of Environmental Medicine, Nagoya University, Nagoya;* [3]*Department of Physiology, Aichi Medical University, Aichi; and* [4]*Gifu University of Medical Science, Gifu, Japan*

Submitted 17 March 2009; accepted in final form 13 May 2009

Kamiya A, Kawada T, Shimizu S, Iwase S, Sugimachi M, Mano T. Slow head-up tilt causes lower activation of muscle sympathetic nerve activity: loading speed dependence of orthostatic sympathetic activation in humans. *Am J Physiol Heart Circ Physiol* 297: H53–H58, 2009. First published May 15, 2009; doi:10.1152/ajpheart.00260.2009.—Many earlier human studies have reported that increasing the tilt angle of head-up tilt (HUT) results in greater muscle sympathetic nerve activity (MSNA) response, indicating the amplitude dependence of sympathetic activation in response to orthostatic stress. However, little is known about whether and how the inclining speed of HUT influences the MSNA response to HUT, independent of the magnitude of HUT. Twelve healthy subjects participated in passive 30° HUT tests at inclining speeds of 1° (control), 0.1° (slow), and 0.0167° (very slow) per second. We recorded MSNA (tibial nerve) by microneurography and assessed nonstationary time-dependent changes of R-R interval variability using a complex demodulation technique. MSNA averaged over every 10° tilt angle increased during inclination from 0° to 30°, with smaller increases in the slow and very slow tests than in the control test. Although a 3-min MSNA overshoot after reaching 30° HUT was observed in the control test, no overshoot was detected in the slow and very slow tests. In contrast with MSNA, increases in heart rate during the inclination and after reaching 30° were similar in these tests, probably because when compared with the control test, greater increases in plasma epinephrine counteracted smaller autonomic responses in the very slow test. These results indicate that slower HUT results in lower activation of MSNA, suggesting that HUT-induced sympathetic activation depends partially on the speed of inclination during HUT in humans.

autonomic nervous system; baroreflex; heart rate variability; microneurography

HUMANS HAVE BEEN SUBJECTED to ceaseless orthostatic stresses since they first evolved and assume an orthostatic posture most of their lives. Thus the maintenance of arterial pressure (AP) under orthostatic stress against gravity-driven fluid shift is of great importance. During standing, gravitational fluid shift toward the lower part of the body (i.e., abdominal vascular bed, lower limbs) would cause severe orthostatic hypotension if not counteracted by compensatory mechanisms (27). Orthostatic sympathetic activation mediated by arterial baroreflex has been considered to be the major compensatory mechanism (2, 26, 27) since denervation of baroreceptor afferents causes profound postural hypotension (30). Therefore, many earlier human studies have recorded muscle sympathetic nerve activity (MSNA) by microneurographic technique and investigated MSNA response to various orthostatic stresses such as head-up tilt (HUT) and lower body negative pressure (LBNP) (1, 5, 24). One of the important findings is that stronger orthostatic stress results in greater MSNA response during incremental HUT (3, 13, 14, 28) and LBNP (17), indicating the amplitude dependence of orthostatic MSNA activation. However, less attention has been paid to the effects of loading speed of orthostatic stress on orthostatic sympathetic activation in humans. Although earlier studies reported that rapid HUT causes dynamic and transient hemodynamic response (33, 34, 36), they did not investigate MSNA. Thus it remains unclear whether and how the inclining speed of HUT affects HUT-induced activation of MSNA (loading speed dependence of orthostatic MSNA activation), independent of the magnitude of HUT. This is an important clinical issue because the speed of upright tilting of each patient's bed would influence his/her autonomic nervous and hemodynamic conditions.

Orthostatic sympathetic activation is mainly mediated by arterial baroreflex control of MSNA, which exhibits high-pass filter dynamic transfer characteristics at least in anesthetized animals such as rabbits (15) and rats (29), indicating that more rapid change of AP results in greater response of MSNA to pressure change (15). Accordingly, we hypothesized that a lower speed of HUT results in less MSNA activation in humans. To test the hypothesis, we performed passive 30° HUT tests at three inclining speeds (1°, 0.1°, and 0.0167°/s) in 12 healthy volunteers. We compared the responses of MSNA measured by microneurography and hemodynamics during these tests.

METHODS

Subjects

The subjects were 12 healthy volunteers (10 males and 2 females) with a mean age (±SE) of 24 ± 5 yr, mean height of 164 ± 11 cm, and mean weight of 58 ± 9 kg. They were carefully screened by medical history, physical examination, complete blood count, blood chemistry analyses, electrocardiogram, and psychological testing. Candidates were excluded if they had evidence of cardiovascular or other disease, smoked tobacco products, took medications, or were obese (body mass index >30 kg/m^2). None of the subjects had experienced spontaneous syncope within the past 5 yr. All had a sedentary lifestyle and were not athletes. All subjects gave informed consent to participate in this study, which was approved by the

Address for reprint requests and other correspondence: A. Kamiya, Dept. of Cardiovascular Dynamics, National Cardiovascular Center Research Institute, 5-7-1 Fujishirodai, Suita, Osaka 565-8565, Japan (e-mail: kamiya@ri.ncvc.go.jp).

Committee of Human Research, Research Institute of Environmental Medicine at Nagoya University.

Measurements

MSNA was measured in our laboratory by the method reported previously (22, 35). Briefly, a tungsten microelectrode (model 26-05-1; Federick Haer and Company, Bowdoinham, ME) was inserted percutaneously into the muscle nerve fascicles of the tibial nerve at the right popliteal fossa without anesthesia. Nerve signals were fed into a preamplifier (Kohno Instruments) with two active band-pass filters set between 500 and 5,000 Hz and were monitored with a loudspeaker. MSNA was identified according to the following discharge characteristics (22, 35): *1*) pulse-synchronous and spontaneous efferent discharges, *2*) afferent activity evoked by tapping of calf muscles but not in response to a gentle skin touch, and *3*) enhanced during phase II of the Valsalva maneuver.

AP was measured continuously using a finger photoplethysmograph (Finapres, Model 2300; Ohmeda, Englewood, CO) at the heart level. Systolic and diastolic AP was measured from the continuous pressure wave. Mean AP was calculated by averaging the pressure within a pulse wave. The finger pressure was confirmed to match intermittent (every minute) brachial AP measured by an automated sphygmomanometer (BP203MII; Nippon Colin, Komaki, Japan). In addition, distance between brachial cuff sensor and carotid sinus was measured in individuals, and AP at the height of carotid sinus level was then calculated by subtracting hydrostatic fluid pressure at each tilt angle from brachial AP. Electrocardiogram (chest lead II) and thermistor respirogram were also recorded continuously. A 20-gauge intravenous catheter was inserted into the antecubital vein in the left forearm to obtain venous blood samples for determination of plasma concentrations of epinephrine, norepinephrine, and arginine vasopressin. Thoracic impedance was measured using an impedance plethysmograph (AI-601G; Nihon Koden) to estimate tilt-induced decreases in thoracic fluid volume (12, 19).

Protocols

We instructed the subjects to refrain from eating for 3 h before the experiments. The experimental room was air-conditioned at a temperature of 26°C. Each subject was requested to remain supine on a tilt table set at 0° horizontally. After the microneurographic MSNA signal was detected and an intravenous catheter was placed, three HUT tests (control, slow, and very slow) were performed on each subject. The three tests were conducted in a random order, with intervals of at least 20 min between tests.

In the control test, the subject remained supine (0°) and rested for at least 20 min. Baseline blood sample was then collected, and baseline recordings of variables including MSNA were done for 10 min. Thereafter, the tilt table was inclined to 30° in a continuous passive manner at a speed of 1°/s. Thus inclination to 30° required 30 s. After reaching 30°, the tilt table was fixed for 8 min. All variables were monitored continuously. After that, a blood sample was again collected.

The slow and very slow tests were performed similarly to the control test except the speed of inclining the tilt table. The tilt table was continuously inclined to 30° at speeds of 0.1 and 0.0167°/s in the slow and very slow tests, respectively. Thus inclination to 30° required 300 s in the slow test and 1,800 s in the very slow test.

These HUT tests were terminated by returning the tilt table to the 0° horizontal position when any of the following incidents was observed: development of presyncope symptoms such as nausea, sweating, yawning, gray out, and dizziness; and progressive reduction in systolic blood pressure to <80 mmHg.

Data Analysis

Full-wave rectified MSNA signals were fed through a resistance-capacitance low-pass filter at a time constant of 0.1 s to obtain the mean voltage neurogram. The signals were then resampled at 200 Hz together with other cardiovascular variables. MSNA bursts were identified, and their areas were calculated using a computer program custom-built by our laboratory. MSNA was expressed as both the rate of integrated activity per minute (burst rate) and the total activity by integrating individual burst area per minute (total MSNA). Since the burst area, and hence also the total MSNA, was dependent on electrode position, they were expressed as arbitrary units (AU) normalized by the individual's baseline values at supine rest (0°) at the first HUT test (the average of total MSNA per minute during the 10 min of supine rest was given 100 AU). The area of each burst during the subsequent HUT tests was normalized to this value.

Time-dependent changes in amplitudes of low frequency (LF; 0.04–0.15 Hz) and high frequency (HF; 0.15–0.35 Hz) components of R-R interval variability were assessed continuously by complex demodulation using a custom-designed computer program (6, 8, 21). The complex demodulation technique is a nonlinear time-domain method of time series analysis suitable for the investigation of nonstationary/unstable oscillations within an assigned frequency band (8, 21). This method provides instantaneous amplitudes and frequencies of the LF and HF components as a function of time (8, 21). The instantaneous amplitude of HF component of R-R interval variability was used as the index of cardiac vagal nerve activity in this study.

Variables except blood data were averaged over every 10 min during 0° supine rest in all HUT tests. The data were averaged over every 10, 100, and 600 s during inclination of the tilt table from 0° to 30° in the control, slow, and very slow HUT tests, respectively, and averaged over every 1 min after reaching 60° HUT position in all HUT tests. In addition, the data were averaged over every 10° tilt angle during the inclining period.

Statistical Analysis

Data are expressed as means ± SE. Repeated-measure ANOVA was used to compare variables among the speed of HUT tests (control, slow, and very slow). When the main effect or interaction term was found to be significant, post hoc comparisons were made using the Sheffe's F procedure. A P value <0.05 was considered statistically significant.

RESULTS

Figure 1 shows the typical MSNA data during the control, slow, and very slow HUT tests in one subject. Although HUT increased MSNA during inclination of the tilt table from 0° to 30° in all three tests, the increase was apparently greater in the control test than in the slow and very slow tests (Fig. 1). Data from all subjects showed that increases in MSNA averaged over tilt angle (every 10° tilt) during inclination were greater in the control test than in the slow and very slow tests (Fig. 2). In the control test, MSNA showed a transient overshoot of 3 min after reaching 30° HUT and then declined gradually to the steady-state level (Fig. 2). In contrast, in the slow and very slow tests, MSNA reached steady-state levels without overshoot (Fig. 2). The steady-state levels were similar among the control, slow, and very slow tests.

Heart rate averaged over tilt angle (every 10° tilt) increased during all HUT tests, with similar increases in all three tests (Fig. 3). Instantaneous frequencies of LF and HF bands for R-R interval variability were 0.09 and 0.25–0.28 Hz, respectively, and were almost constant during all HUT tests. The LF amplitude of R-R interval variability did not change in any tests (Fig. 3). Of note, although the HF amplitude of R-R interval variability decreased during inclination of the tilt table from 0° to 30°, the decrease averaged over tilt angle was smaller in the

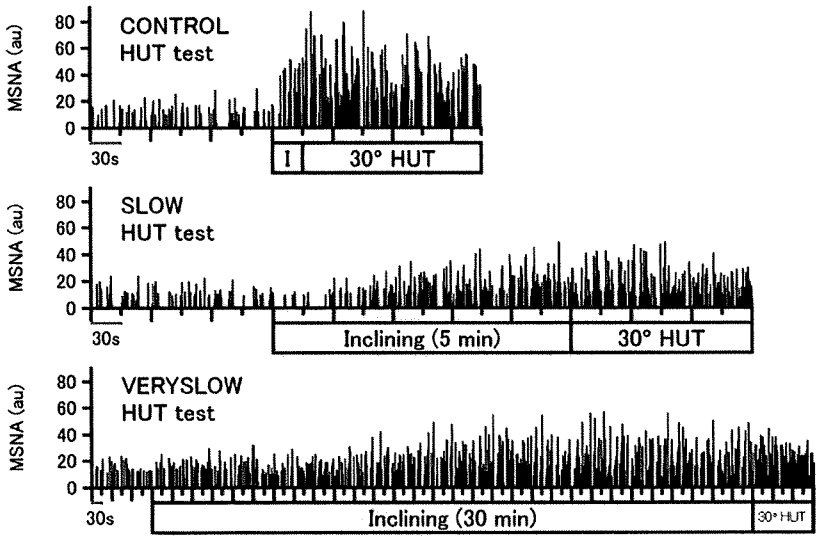

Fig. 1. Representative muscle sympathetic nerve activity (MSNA; integrated signals) data during control (*top*), slow (*middle*), and very slow (*bottom*) head-up tilt (HUT) tests in 1 subject. I (*top*), period of inclination of the tilt bed from 0° supine to 30° HUT posture at an inclining speed of 1°/s. Inclining (*middle* and *bottom*), period of inclination of the tilt bed at speeds of 0.1 and 0.0167°/s, respectively. au, Arbitrary units.

very slow test than in the control and slow tests (Fig. 3). Moreover, the HF amplitude of R-R interval variability reached steady-state levels after reaching 30° HUT, and the level was higher in the very slow test than in the control and slow tests (Fig. 3). Respiratory rate did not change in any tests (Fig. 3).

Systolic AP at the height of brachial level did not change, whereas diastolic AP at the level slightly increased during HUT in the control, slow, and very slow tests. However, there were no differences in both brachial systolic and diastolic APs among the control, slow, and very slow tests (Fig. 4). When AP at the height of carotid sinus level was predicted by subtracting hydrostatic fluid pressure at each tilt angle from brachial AP, systolic and diastolic AP at the carotid sinus level decreased during HUT similarly in the control, slow, and very slow tests (Fig. 4). Thoracic impedance increased during all HUT tests, and the changes averaged over tilt angle were almost identical in all three tests (Fig. 4).

When compared with the 0° supine level, plasma epinephrine concentration increased at the end of HUT tests, with greater increase in the very slow test (from 25.3 ± 3.7 to

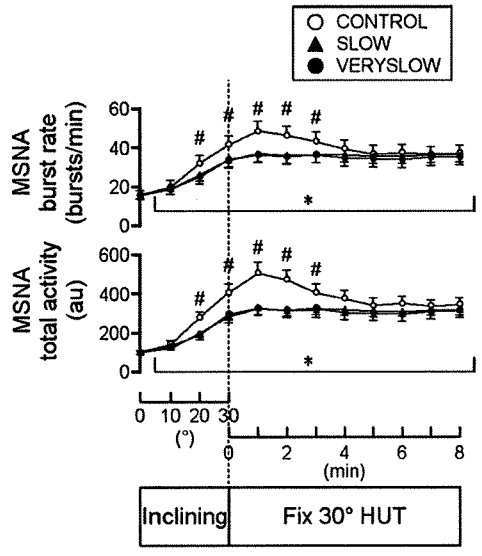

Fig. 2. MSNA burst rate and total activity during control (○), slow (▲), and very slow (●) HUT tests. The *x*-axis to the left of the vertical dotted line indicates that data are averaged over every 10° tilt angle during inclination from 0° supine to 30° HUT, and the *x*-axis to the right of the dotted line indicates that data are averaged over every 1 min after reaching 30° HUT. #$P < 0.05$ vs. slow and very slow tests; *$P < 0.05$ vs. 0° supine. Error bars denote SE.

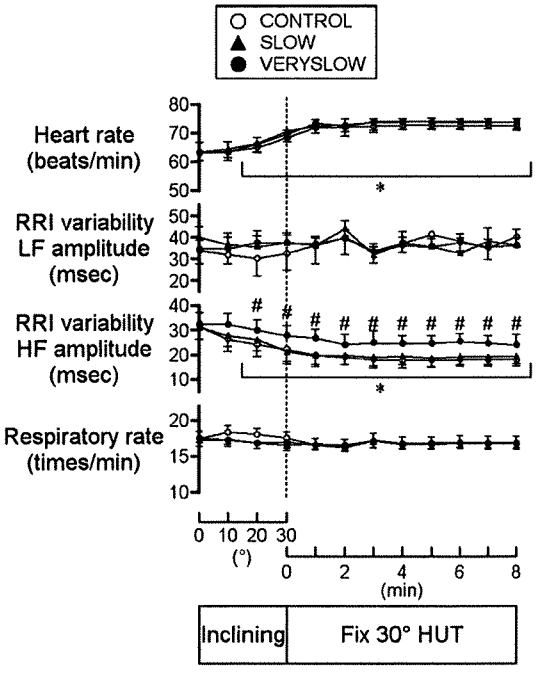

Fig. 3. Heart rate, amplitude of low frequency (LF) and high frequency (HF) component of R-R interval (RRI) variability, and respiratory rate during control (○), slow (▲), and very slow (●) HUT tests. The *x*-axis to the left of the vertical dotted line indicates that data are averaged over every 10° tilt angle during inclination from 0° supine to 30° HUT, and the *x*-axis to the right of the dotted line indicates that data are averaged over every 1 min after reaching 30° HUT. #$P < 0.05$ vs. control and slow tests; *$P < 0.05$ vs. 0° supine posture. Error bars denote SE.

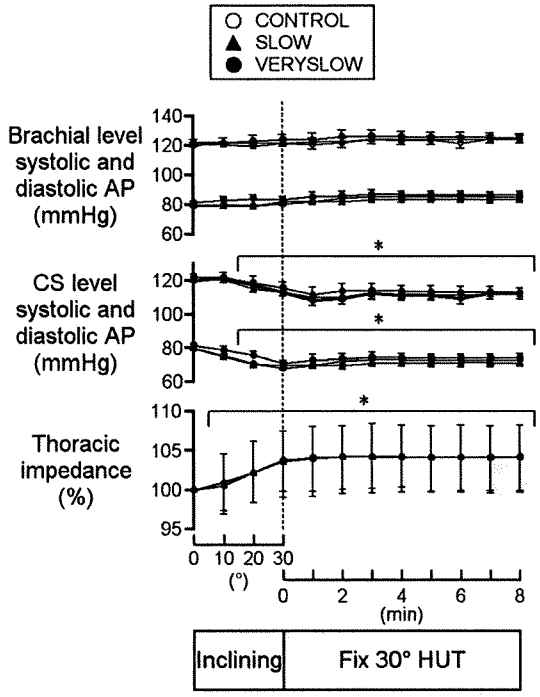

Fig. 4. Systolic and diastolic arterial pressure (AP) measured at the height of brachial level and predicted at the height of carotid sinus (CS) level, and thoracic impedance (percentage of baseline value at 0° supine) during control (○), slow (▲), and very slow (●) HUT tests. The *x*-axis to the left of the vertical dotted line indicates that data are averaged over every 10° tilt angle during inclination from 0° supine to 30° HUT, and the *x*-axis to the right of the dotted line indicates that data are averaged over every 1 min after reaching 30° HUT. $*P < 0.05$ vs. 0° supine posture. Error bars denote SE.

49.3 ± 7.4 pg/ml) than in the control (from 25.8 ± 4.0 to 35.1 ± 5.3 pg/ml) and slow (from 24.3 ± 3.5 to 36.0 ± 5.0 pg/ml) tests. Plasma norepinephrine concentration increased at the end of HUT tests similarly in the control (from 132.2 ± 10.4 to 180.2 ± 11.4 pg/ml), slow (from 134.0 ± 9.2 to 176.5 ± 9.8 pg/ml), and very slow (from 134.2 ± 10.7 to 179.4 ± 9.4 pg/ml) tests. Plasma arginine vasopressin concentration increased at the end of HUT tests similarly in the control (from 3.6 ± 0.4 to 3.9 ± 0.4 pg/ml), slow (from 3.6 ± 0.4 to 3.9 ± 0.4 pg/ml), and very slow (from 3.7 ± 0.4 to 4.0 ± 0.4 pg/ml) tests.

DISCUSSION

Speed Dependence of Orthostatic MSNA Activation

Many earlier human studies have reported that HUT at a larger tilt angle results in greater MSNA response, indicating the amplitude dependence of sympathetic activation in response to orthostatic stress. However, little is known about whether and how the inclining speed during HUT influences MSNA response to HUT, independent of the magnitude of HUT. Our major findings of the present study are that *1*) MSNA averaged over tilt angle increases during inclination of the tilt table from 0° to 30°, with smaller increase in the slow (0.1°/s) and very slow (0.0167°/s) tests than in the control tests (1°/s) and *2*) although a 3-min MSNA overshoot after reaching 30° HUT was observed in the control test, no overshoot was found in the slow and very slow tests. These results support our hypothesis that a lower speed of HUT results in less MSNA activation in humans, indicating the loading speed dependence of orthostatic MSNA activation. The speed-dependent sympathetic activation would contribute to prevent hypotension and maintain AP during rapid postural change from supine to upright posture.

Possible Mechanisms for the Speed Dependence of Orthostatic MSNA Activation

Since the HUT activates multiple physiological mechanisms, it is difficult to strictly determine the primary input to humans during postural change from the supine to upright postures. Therefore, we cannot conclude the true mechanisms for the speed dependence of orthostatic MSNA activation observed in this study. In this study, HUT decreased AP at the height of carotid sinus level decreased and increased thoracic impedance. We thus challenged to discuss possible relations of arterial and cardiopulmonary baroreflexes with the speed dependence of orthostatic MSNA activation.

Arterial baroreflex. Although arterial baroreflex is the major mechanism that increases sympathetic nerve activity (SNA) and maintains AP under orthostatic stress (2, 26, 27), it has high-pass filter dynamic transfer characteristics from baroreceptor pressure input to SNA. The high-pass filter characteristics have been investigated in detail by baroreflex open-loop experiments in anesthetized animals such as rabbits (11, 15) and rats (29). This indicates that more rapid change of AP resulted in greater response of SNA to pressure change. In addition, the high-pass filter characteristics might also be observed in earlier human study (10), since MSNA increased/decreased and turned to partially decrease/increase in response to stepwise neck pressure/suction. Although transfer function was not calculated in the study, the SNA response in humans may be consistent with the MSNA response (initial drop and partial recover) to stepwise increase in baroreceptor pressure in anesthetized animals (15) and suggests that the arterial baroreflex control of SNA in humans would also have the high-pass filter characteristics.

One possible mechanism for the lower MSNA during inclination in slower HUT tests is the high-pass filter characteristics of the arterial baroreflex control of SNA. Since the decreases in AP predicted at the height of carotid sinus level over tilt angle were similar in the control, slow, and very slow HUT tests, we assumed that the tilt-induced pressure perturbation was similar in the three HUT tests except for the speed. However, the high-pass filter characteristics of the arterial baroreflex control of SNA (11, 15, 16) would cause greater response of SNA to pressure change in the control HUT test that induced more rapid decreases in AP than the slow and very slow HUT tests. Of note, the dynamic transfer characteristics could not explain a few minutes of overshoot of MSNA activation after reaching 30° HUT posture observed in the control HUT test. Other mechanisms would be responsible for the overshoot of orthostatic MSNA response in faster HUT test.

Cardiopulmonary baroreflex. In addition to arterial baroreflex, cardiopulmonary baroreflex is known to mediate orthostatic activation of SNA. In our results, at a tilt angle of 10°, thoracic impedance increased similarly in control, slow, and very slow tests, indicating that the gravitational fluid shift directed toward the lower part of the body (such as the abdominal vascular bed and lower limbs) may be similar in all

three tests. In addition, MSNA increased at the tilt angle of 10° similarly in control, slow, and very slow tests, but AP predicted at the height of carotid sinus level did not change. These results suggest that cardiopulmonary baroreflex was activated by 10° HUT similarly in these tests and mediated similar magnitude of orthostatic MSNA activation but did not induce speed-dependent differentiation of MSNA. Therefore, it is possible that cardiopulmonary baroreflex control of MSNA does not have high-pass filter characteristics. However, since even small HUT can activate not only cardiopulmonary but also arterial baroreflexes similarly to low levels (i.e., −10 and −15 mmHg) of lower body negative pressure (4), it is difficult to isolate these baroreflexes and to conclude regarding the relation between cardiopulmonary baroreflex and the speed dependence of orthostatic MSNA activation in HUT. In addition, it was reported that cardiopulmonary and arterial baroreceptor afferents interact in a sense of a nonadditive attenuation (25).

Other mechanisms. Mechanisms other than baroreflexes might be responsible for the speed dependence of orthostatic MSNA activation. The first possibility is the vestibulosympathetic reflex, which may be involved in mediating pressor and sympathetic responses to orthostatic stress in rats (23) and humans (31). Since the reflex may be engaged differentially in the control versus the slow and very slow HUT tests, it can relate with the speed dependence of orthostatic MSNA activation observed in this study. The second possibility is the stroke volume, which had a close correlation with MSNA in their changes by orthostatic stress (20), although the neural pathway connecting stroke volume to MSNA may be unclear. Finally, humoral substances can relate with smaller activation of MSNA in the very slow HUT tests. In this study, increases in plasma epinephrine, not norepinephrine and arginine vasopressin, were greater in the very slow test than the control test.

Speed Independence of Orthostatic Tachycardia in the Present Study

In contrast with MSNA, orthostatic tachycardia is independent of inclining speed of HUT. The results may be consistent with a early study (32) that addressed more rapid HUT (i.e., 70° or 90° passive HUT in 3 s, and 70° passive HUT in 1.5 s) and reported that speed of HUT did not affect on initial heart rate responses to rapid HUT. It is difficult to understand the mechanisms for the finding. If baroreflex control of cardiac SNA is similar to that of MSNA as observed in rabbits (15), it is expected that the very slow test mediates a smaller increase in heart rate during inclination than the control test. This raises a possibility that mechanisms other than sympathetic control counteract the speed dependence of orthostatic sympathetic activation and result in speed-independent orthostatic tachycardia. Although we cannot measure cardiac vagal nerve activity in humans, there is a well-known, hypothetical consideration that the HF amplitude of R-R interval variability can reflect respiratory modulation of cardiac vagal nerve activity (7, 9). If so, our results suggest that the decrease in the index of cardiac vagal nerve activity averaged over tilt angle during inclination of HUT was smaller in the very slow HUT test than in the control test (indicating the speed dependence of orthostatic cardiac vagal suppression). Therefore, the speed independence of orthostatic tachycardia in the present study cannot be explained by autonomic neural controls. One possible explanation is that greater increase in plasma epinephrine counteracted the smaller response of sympathetic and, probably, vagal nerve activities.

Limitations

This study has several limitations. First, we used a mild to moderate HUT test (30°) in this study. Sequential HUT tests were necessary for this study, but sequential HUT tests at greater tilt angles (>60°) pose a problem in keeping constant electrode positions for microneurography and maintaining the quality of MSNA recording. Second, since we focused on the effects of slow-speed HUT on orthostatic MSNA response, we used inclining speeds of 1, 0.1, and 0.0167°/s in HUT tests. Finally, the HF amplitude of R-R interval variability is a limited measure of cardiac vagal control in the human (18), although we used it as an index of cardiac vagal modulation in the discussion.

In conclusion, although HUT at an inclining speed of 1°/s causes high MSNA activation with an overshoot of a few minutes, slower HUT (0.1 and 0.0167°/s) results in lower MSNA activation. This indicates that that HUT-induced sympathetic activation depends partially on the tilting speed in humans.

GRANTS

This study was supported by the research project promoted by Ministry of Health, Labour and Welfare in Japan (H18-nano-ippan-003 and H21-nano-ippan-005), the Grants-in-Aid for Scientific Research promoted by Ministry of Education, Culture, Sports, Science and Technology in Japan (20390462), and the Industrial Technology Research Grant Program from New Energy and Industrial Technology Development Organization of Japan (06B44524a).

REFERENCES

1. **Cooke WH, Hoag JB, Crossman AA, Kuusela TA, Tahvanainen KU, Eckberg DL.** Human responses to upright tilt: a window on central autonomic integration. *J Physiol* 517: 617–628, 1999.
2. **Eckberg DL, Sleight P.** *Human baroreflexes in Health and Disease.* New York: Oxford Univ. Press, 1992, p. 3–299.
3. **Fu Q, Okazaki K, Shibata S, Shook RP, Vangunday TB, Galbreath MM, Reelick MF, Levine BD.** Menstrual cycle effects on sympathetic neural responses to upright tilt. *J Physiol* 587: 2019–2031, 2009.
4. **Fu Q, Shibata S, Hastings JL, Prasad A, Palmer MD, Levine BD.** Evidence for unloading arterial baroreceptors during low levels of lower body negative pressure in humans. *Am J Physiol Heart Circ Physiol* 296: H480–H488, 2009.
5. **Furlan R, Porta A, Costa F, Tank J, Baker L, Schiavi R, Robertson D, Malliani A, Mosqueda-Garcia R.** Oscillatory patterns in sympathetic neural discharge and cardiovascular variables during orthostatic stimulus. *Circulation* 101: 886–892, 2000.
6. **Hayano J, Mukai S, Fukuta H, Sakata S, Ohte N, Kimura G.** Postural response of low-frequency component of heart rate variability is an increased risk for mortality in patients with coronary artery disease. *Chest* 120: 1942–1952, 2001.
7. **Hayano J, Sakakibara Y, Yamada A, Yamada M, Mukai S, Fujinami T, Yokoyama K, Watanabe Y, Takata K.** Accuracy of assessment of cardiac vagal tone by heart rate variability in normal subjects. *Am J Cardiol* 67: 199–204, 1991.
8. **Hayano J, Taylor JA, Yamada A, Mukai S, Hori R, Asakawa T, Yokoyama K, Watanabe Y, Takata K, Fujinami T.** Continuous assessment of hemodynamic control by complex demodulation of cardiovascular variability. *Am J Physiol Heart Circ Physiol* 264: H1229–H1238, 1993.
9. **Hayano J, Yasuma F.** Hypothesis: respiratory sinus arrhythmia is an intrinsic resting function of cardiopulmonary system. *Cardiovasc Res* 58: 1–9, 2003.
10. **Ichinose M, Saito M, Kitano A, Hayashi K, Kondo N, Nishiyasu T.** Modulation of arterial baroreflex dynamic response during mild orthostatic stress in humans. *J Physiol* 557: 321–330, 2004.

11. **Ikeda Y, Kawada T, Sugimachi M, Kawaguchi O, Shishido T, Sato T, Miyano H, Matsuura W, Alexander J Jr, Sunagawa K.** Neural arc of baroreflex optimizes dynamic pressure regulation in achieving both stability and quickness. *Am J Physiol Heart Circ Physiol* 271: H882–H890, 1996.
12. **Iwase S, Mano T, Cui J, Kitazawa H, Kamiya A, Miyazaki S, Sugiyama Y, Mukai C, Nagaoka S.** Sympathetic outflow to muscle in humans during short periods of microgravity produced by parabolic flight. *Am J Physiol Regul Integr Comp Physiol* 277: R419–R426, 1999.
13. **Iwase S, Mano T, Watanabe T, Saito M, Kobayashi F.** Age-related changes of sympathetic outflow to muscles in humans. *J Gerontol* 46: M1–M5, 1991.
14. **Kamiya A, Iwase S, Sugiyama Y, Mano T, Sudoh M.** Vasomotor sympathetic nerve activity in men during bed rest and on orthostasis after bed rest. *Aviat Space Environ Med* 71: 142–149, 2000.
15. **Kamiya A, Kawada T, Yamamoto K, Michikami D, Ariumi H, Miyamoto T, Shimizu S, Uemura K, Aiba T, Sunagawa K, Sugimachi M.** Dynamic and static baroreflex control of muscle sympathetic nerve activity (SNA) parallels that of renal and cardiac SNA during physiological change in pressure. *Am J Physiol Heart Circ Physiol* 289: H2641–H2648, 2005.
16. **Kawada T, Zheng C, Yanagiya Y, Uemura K, Miyamoto T, Inagaki M, Shishido T, Sugimachi M, Sunagawa K.** High-cut characteristics of the baroreflex neural arc preserve baroreflex gain against pulsatile pressure. *Am J Physiol Heart Circ Physiol* 282: H1149–H1156, 2002.
17. **Khan MH, Sinoway LI, MacLean DA.** Effects of graded LBNP on MSNA and interstitial norepinephrine. *Am J Physiol Heart Circ Physiol* 283: H2038–H2044, 2002.
18. **Kollai M, Mizsei G.** Respiratory sinus arrhythmia is a limited measure of cardiac parasympathetic control in man. *J Physiol* 424: 329–342, 1990.
19. **Kubicek WG, From AH, Patterson RP, Witsoe DA, Castaneda A, Lillehei RC, Ersek R.** Impedance cardiography as a noninvasive means to monitor cardiac function. *J Assoc Adv Med Instrum* 4: 79–84, 1970.
20. **Levine BD, Pawelczyk JA, Ertl AC, Cox JF, Zuckerman JH, Diedrich A, Biaggioni I, Ray CA, Smith ML, Iwase S, Saito M, Sugiyama Y, Mano T, Zhang R, Iwasaki K, Lane LD, Buckey JC Jr, Cooke WH, Baisch FJ, Eckberg DL, Blomqvist CG.** Human muscle sympathetic neural and haemodynamic responses to tilt following spaceflight. *J Physiol* 538: 331–340, 2002.
21. **Lipsitz LA, Hayano J, Sakata S, Okada A, Morin RJ.** Complex demodulation of cardiorespiratory dynamics preceding vasovagal syncope. *Circulation* 98: 977–983, 1998.
22. **Mano T.** Microneurography as a tool to investigate sympathetic nerve responses to environmental stress. *Aviakosm Ekolog Med* 31: 8–14, 1997.
23. **Matsuda T, Gotoh TM, Tanaka K, Gao S, Morita H.** Vestibulosympathetic reflex mediates the pressor response to hypergravity in conscious rats: contribution of the diencephalon. *Brain Res* 1028: 140–147, 2004.
24. **Mosqueda-Garcia R, Furlan R, Tank J, Fernandez-Violante R.** The elusive pathophysiology of neurally mediated syncope. *Circulation* 102: 2898–2906, 2000.
25. **Persson P, Ehmke H, Kirchheim H, Seller H.** The influence of cardiopulmonary receptors on long-term blood pressure control and plasma renin activity in conscious dogs. *Acta Physiol Scand* 130: 553–561, 1987.
26. **Persson P, Kirchheim H.** *Baroreceptor reflexes: integrative functions and clinical aspects.* Berlin: Springer-Verlag, 1991.
27. **Rowell LB.** *Human cardiovascular control.* New York: Oxford Univ. Press, 1993, p. 3–254.
28. **Saito M, Foldager N, Mano T, Iwase S, Sugiyama Y, Oshima M.** Sympathetic control of hemodynamics during moderate head-up tilt in human subjects. *Environ Med* 41: 151–155, 1997.
29. **Sato T, Kawada T, Inagaki M, Shishido T, Sugimachi M, Sunagawa K.** Dynamics of sympathetic baroreflex control of arterial pressure in rats. *Am J Physiol Regul Integr Comp Physiol* 285: R262–R270, 2003.
30. **Sato T, Kawada T, Sugimachi M, Sunagawa K.** Bionic technology revitalizes native baroreflex function in rats with baroreflex failure. *Circulation* 106: 730–734, 2002.
31. **Sauder CL, Leonard TO, Ray CA.** Greater sensitivity of the vestibulosympathetic reflex in the upright posture in humans. *J Appl Physiol* 105: 65–69, 2008.
32. **Sprangers RL, Veerman DP, Karemaker JM, Wieling W.** Initial circulatory responses to changes in posture: influence of the angle and speed of tilt. *Clin Physiol* 11: 211–220, 1991.
33. **Sundkvist G, Lilja B.** Effect of the degree and speed of tilt on the immediate heart rate reaction. *Clin Physiol* 3: 381–386, 1983.
34. **Toska K, Walloe L.** Dynamic time course of hemodynamic responses after passive head-up tilt and tilt back to supine position. *J Appl Physiol* 92: 1671–1676, 2002.
35. **Wallin BG, Fagius J.** Peripheral sympathetic neural activity in conscious humans. *Annu Rev Physiol* 50: 565–576, 1988.
36. **Wong BJ, Sheriff DD.** Myogenic origin of the hypotension induced by rapid changes in posture in awake dogs following autonomic blockade. *J Appl Physiol* 105: 1837–1844, 2008.

Am J Physiol Heart Circ Physiol 296: H1666–H1674, 2009.
First published February 27, 2009; doi:10.1152/ajpheart.01041.2008.

Angiotensin II disproportionally attenuates dynamic vagal and sympathetic heart rate controls

Toru Kawada,[1] Masaki Mizuno,[1] Shuji Shimizu,[2] Kazunori Uemura,[1] Atsunori Kamiya,[1] and Masaru Sugimachi[1]

[1]*Department of Cardiovascular Dynamics, Advanced Medical Engineering Center, National Cardiovascular Center Research Institute, Osaka and* [2]*Japan Association for the Advancement of Medical Equipment, Tokyo, Japan*

Submitted 29 September 2008; accepted in final form 25 February 2009

Kawada T, Mizuno M, Shimizu S, Uemura K, Kamiya A, Sugimachi M. Angiotensin II disproportionally attenuates dynamic vagal and sympathetic heart rate controls. *Am J Physiol Heart Circ Physiol* 296: H1666–H1674, 2009. First published February 27, 2009; doi:10.1152/ajpheart.01041.2008.—To better understand the pathophysiological role of angiotensin II (ANG II) in the dynamic autonomic regulation of heart rate (HR), we examined the effects of intravenous administration of ANG II (10 $\mu g \cdot kg^{-1} \cdot h^{-1}$) on the transfer function from vagal or sympathetic nerve stimulation to HR in anesthetized rabbits with sinoaortic denervation and vagotomy. In the vagal stimulation group (n = 7), we stimulated the right vagal nerve for 10 min using binary white noise (0–10 Hz). The transfer function from vagal stimulation to HR approximated a first-order low-pass filter with pure delay. ANG II attenuated the dynamic gain from 7.6 ± 0.9 to 5.8 ± 0.9 $beats \cdot min^{-1} \cdot Hz^{-1}$ (means ± SD; $P < 0.01$) without affecting the corner frequency or pure delay. In the sympathetic stimulation group (n = 7), we stimulated the right postganglionic cardiac sympathetic nerve for 20 min using binary white noise (0–5 Hz). The transfer function from sympathetic stimulation to HR approximated a second-order low-pass filter with pure delay. ANG II slightly attenuated the dynamic gain from 10.8 ± 2.6 to 10.2 ± 3.1 $beats \cdot min^{-1} \cdot Hz^{-1}$ ($P = 0.049$) without affecting the natural frequency, damping ratio, or pure delay. The disproportional suppression of the dynamic vagal and sympathetic regulation of HR would result in a relative sympathetic predominance in the presence of ANG II. The reduced high-frequency component of HR variability in patients with cardiovascular diseases, such as myocardial infarction and heart failure, may be explained in part by the peripheral effects of ANG II on the dynamic autonomic regulation of HR.

systems analysis; transfer function; heart rate variability; cardiac sympathetic nerve activity; rabbit

AUTONOMIC NERVOUS ACTIVITY changes dynamically during daily activity, and thus the dynamic heart rate (HR) regulation by the autonomic nervous system is physiologically important. The high-frequency (HF) component of HR variability (HRV) is thought to reflect primarily vagal nerve activity, because the vagal nerve can change the HR more quickly than the sympathetic nerve (1, 3, 14, 34). This does not mean, however, that the sympathetic system cannot affect the HF component. For example, an increase in background sympathetic tone augments the HR response to vagal stimulation, an effect that has been referred to as accentuated antagonism (20). In accordance with accentuated antagonism, selective cardiac sympathetic nerve stimulation augments the dynamic HR response to vagal stimulation (14). On the other hand, high plasma concentration of norepinephrine (NE) with no direct activation of the cardiac sympathetic nerve attenuates the dynamic HR response to vagal stimulation via an α-adrenergic mechanism (24). These results suggest that the sympathetic system can influence the HF component via complex interactions with the vagal system.

During systemic sympathetic activation, the renin-angiotensin system is activated through stimulation of β_1-adrenergic receptors on juxtaglomerular granular cells (8, 12). In such conditions as hypertension, myocardial ischemia, and heart failure, the renin-angiotensin system and the sympathetic nervous system are both activated (9, 35). Previous studies demonstrated that acute intravenous or intracerebroventricular administration (32) or chronic intravenous administration of angiotensin II (ANG II) modified the baroreflex control of HR in rabbits (5), possibly via a decrease in vagal tone and an increase in sympathetic tone to the heart. In the present study, we focused on the peripheral effects of ANG II and examined the effects of intravenous ANG II on the dynamic HR response to vagal or postganglionic cardiac sympathetic nerve stimulation. In a previous study from our laboratory where anesthetized cats were used, intravenous ANG II (10 $\mu g \cdot kg^{-1} \cdot h^{-1}$) attenuated myocardial interstitial acetylcholine (ACh) release in response to vagal nerve stimulation (17); therefore, we hypothesized that intravenous ANG II at this dose would attenuate the dynamic HR response to vagal nerve stimulation. On the other hand, a previous study from our laboratory where anesthetized rabbits were used demonstrated that intravenous ANG II at a similar dose of 6 $\mu g \cdot kg^{-1} \cdot h^{-1}$ did not affect the peripheral arc transfer function estimated between renal sympathetic nerve activity and arterial pressure (AP) (13). Accordingly, we hypothesized that intravenous administration of ANG II would not modulate the dynamic sympathetic control of HR significantly. We focused on the relative effects of ANG II on the vagal and sympathetic HR regulations because the balance between vagal and sympathetic nerve activities would be a key to understanding the pathophysiology of several cardiovascular diseases.

MATERIALS AND METHODS

Surgical preparations. Animal care was performed in accordance with *Guideline Principles for the Care and Use of Animals in the Field of Physiological Sciences*, which has been approved by the Physiological Society of Japan. All experimental protocols were reviewed and approved by the Animal Subjects Committee at the National Cardiovascular Center. Twenty-one Japanese white rabbits weighing 2.4–3.4 kg were anesthetized with intravenous injections (2 ml/kg) of a mixture of urethane (250 mg/ml) and α-chloralose (40 mg/ml) and mechanically ventilated with oxygen-enriched room air. A double-lumen catheter was inserted into the right femoral vein, and a supplemental dose of the anesthetics was given continuously (0.5–1.0

Address for reprint requests and other correspondence: T. Kawada, Dept. of Cardiovascular Dynamics, Advanced Medical Engineering Center, National Cardiovascular Center Research Institute, 5-7-1 Fujishirodai, Suita, Osaka 565-8565, Japan (e-mail: torukawa@res.ncvc.go.jp).

$ml \cdot kg^{-1} \cdot h^{-1}$). AP was monitored using a micromanometer catheter (Millar Instruments, Houston, TX) inserted into the right femoral artery. HR was determined from the electrocardiogram using a cardiotachometer. Sinoaortic denervation and vagotomy were performed bilaterally to minimize reflex changes in efferent sympathetic nerve activity. The left and right cardiac sympathetic nerves were exposed using a midline thoracotomy and sectioned (16). In the vagal stimulation group, a pair of bipolar stainless steel wire electrodes was attached to the cardiac end of the sectioned right vagal nerve for stimulation. A pair of stainless steel wire electrodes was attached to the proximal end of the sectioned right cardiac sympathetic nerve for recording efferent cardiac sympathetic nerve activity (CSNA). In the sympathetic stimulation group, a pair of bipolar stainless steel wire electrodes was attached to the cardiac end of the sectioned right sympathetic nerve for stimulation. Efferent CSNA was recorded from the proximal end of the sectioned left cardiac sympathetic nerve. The preamplified nerve signal was band-pass filtered between 150 and 1,000 Hz. The signal was then full-wave rectified and low-pass filtered with a cut-off frequency of 30 Hz to quantify the nerve activity. Both the stimulation and recording electrodes were fixed to the nerve by addition-curing silicone glue (Kwik-Sil; World Precision Instruments, Sarasota, FL). We confirmed that the recorded CSNA was mainly postganglionic by observing the disappearance of CSNA following intravenous administration of hexamethonium bromide (50 mg/kg) at the end of each experiment. The body temperature of the animal was maintained at 38°C with a heating pad throughout the experiment.

Protocols. In the vagal stimulation group ($n = 7$), the stimulation amplitude was adjusted (3–6 V) in each animal to yield a HR decrease of ~50 beats/min at 5-Hz tonic stimulation with a pulse duration of 2 ms. To estimate the transfer function from vagal stimulation to HR, a random vagal stimulus was applied for 10 min by altering the stimulus command every 500 ms at either 0 or 10 Hz according to a binary white noise signal. The input power spectral density was relatively constant up to 1 Hz, which covered the upper frequency range of interest with respect to the vagal transfer function in rabbits (26).

In the sympathetic stimulation group ($n = 7$), the stimulation amplitude was adjusted (1–3 V) in each animal to yield a HR increase of ~50 beats/min at 5-Hz tonic stimulation with a pulse duration of 2 ms. To estimate the transfer function from sympathetic stimulation to HR, a random sympathetic stimulus was applied for 20 min by altering the stimulus command every 2 s at either 0 or 5 Hz according to a binary white noise signal. The input power spectral density was relatively constant up to 0.25 Hz, which covered the upper frequency range of interest with respect to the sympathetic transfer function in rabbits (15).

In both the vagal stimulation and sympathetic stimulation groups, the dynamic HR response to nerve stimulation was first recorded under conditions of continuous intravenous infusion of physiological saline solution ($1\ ml \cdot kg^{-1} \cdot h^{-1}$). After the control data were recorded, nerve stimulation was stopped and ANG II was intravenously administered at $10\ \mu g \cdot kg^{-1} \cdot h^{-1}$ ($1\ ml \cdot kg^{-1} \cdot h^{-1}$ of 10 μg/ml solution) instead of the physiological saline solution. After 15 min, we repeated the random stimulation of the vagal or sympathetic nerve while continuing the intravenous injection of ANG II. We used the same binary white noise sequence for the control and ANG II conditions in each animal and changed the sequence for different animals.

In a supplemental protocol ($n = 7$), we examined the time effect on the estimation of the sympathetic transfer function. The 20-min random sympathetic stimulation was repeated twice with an intervening interval of more than 20 min.

Data analysis. Data were digitized at 200 Hz using a 16-bit analog-to-digital converter and stored on the hard disk of a dedicated laboratory computer system. Prestimulation values of HR, AP, and CSNA were calculated by averaging data obtained during the 10 s immediately before nerve stimulation. The mean HR and AP values in response to nerve stimulation were calculated by averaging data obtained during the nerve stimulation period. The mean level of CSNA during the nerve stimulation period was not evaluated because contamination from stimulation artifacts could not be completely eliminated.

The transfer function from nerve stimulation to the HR response was estimated as follows. The input-output data pairs of nerve stimulation and HR were resampled at 10 Hz. To avoid the initial transition from no stimulation to random stimulation biased the transfer function estimation, data were processed only from 2 min after the initiation of random stimulation. In the vagal stimulation group, the data were divided into eight segments of 1,024 data points that half-overlapped with neighboring segments. In the sympathetic stimulation group, the data were divided into eight segments of 2,048 data points that half-overlapped with neighboring segments. For each segment, a linear trend was subtracted and a Hanning window was applied. We then performed a fast Fourier transformation to obtain the frequency spectra of the stimulation command [$X(f)$] and HR [$HR(f)$] (4). We calculated ensemble averages of the power spectral densities of the stimulation command [$S_{X \cdot X}(f)$] and HR [$S_{HR \cdot HR}(f)$] and the cross spectral density between the two signals [$S_{HR \cdot X}(f)$]. Finally, we obtained the transfer function [$H(f)$] from the nerve stimulation to HR response using the following equation (23):

$$H(f) = \frac{S_{HR \cdot X}(f)}{S_{X \cdot X}(f)}$$

To quantify the linear dependence of the HR response to vagal or sympathetic nerve stimulation, we estimated the magnitude-squared coherence function [$Coh(f)$] using the following equation (23):

$$Coh(f) = \frac{|S_{HR \cdot X}(f)|^2}{S_{X \cdot X}(f) \cdot S_{HR \cdot HR}(f)}$$

The coherence function ranges zero and unity and indicates a frequency-domain measure of linear dependence between input and output variables.

Because previous studies found that the transfer function from vagal stimulation to HR approximated a first-order low-pass filter with pure delay (14, 24), we determined the parameters of the vagal transfer function using the following model:

$$H_{vagus}(f) = -\frac{K}{1 + \frac{f}{f_C} j} e^{-2\pi f j L}$$

where K is dynamic gain (in $beats \cdot min^{-1} \cdot Hz^{-1}$), f_C is the corner frequency (in Hz), and L is pure delay (in s). Variables f and j represent frequency and an imaginary unit, respectively. The minus sign in the right side of the equation corresponds to the negative HR response to vagal stimulation.

Because previous studies suggested that the transfer function from sympathetic stimulation to HR approximated a second-order low-pass filter with pure delay (14, 28), we determined the parameters of the sympathetic transfer function using the following model:

$$H_{symp}(f) = \frac{K}{1 + 2\zeta \frac{f}{f_N} j + \left(\frac{f}{f_N} j\right)^2} e^{-2\pi f j L}$$

where K is dynamic gain (in $beats \cdot min^{-1} \cdot Hz^{-1}$), f_N is the natural frequency (in Hz), ζ is the damping ratio, and L is pure delay (in s).

Because deviation of the model transfer function [$H_{model}(f)$] from the estimated transfer function [$H_{est}(f)$] would affect the transfer function parameters, we assessed the goodness of fit using the following equation:

$$\text{Goodness of Fit (\%)} = 100 \times \left[1 - \left(\sum_{m=1}^{N} \frac{|H_{model}(f) - H_{est}(f)|^2}{m}\right) \Big/ \left(\sum_{m=1}^{N} \frac{|H_{est}(f)|^2}{m}\right)\right]$$

$$f = f_0 \times m$$

where f_0, m, and N represent the fundamental frequency of the Fourier transformation, a frequency index, and the number of data points used for the fitting, respectively. When $H_{model}(f)$ is zero for all of the frequencies, the goodness of fit is zero. When $H_{model}(f)$ equals $H_{est}(f)$ for all of the frequencies, the goodness of fit is 100%.

To facilitate intuitive understanding of the dynamic characteristics described by the transfer function (see Appendix A for details), we calculated the step response from the corresponding transfer function as follows. An impulse response of the system was calculated using the inverse Fourier transformation of the estimated transfer function. The step response was then obtained from the time integral of the impulse response. The steady-state response was calculated by averaging the last 10 s of data from the step response. The 80% rise time for the sympathetic step response or the 80% fall time for the vagal step response was estimated as the time at which the step response reached 80% of the steady-state response.

Statistics. All data are presented as means and SD values. Mean values of HR, AP, and CSNA as well as parameters of the transfer functions and step responses were compared between the control and ANG II conditions using paired *t*-tests. Differences were considered significant when $P < 0.05$ (11).

RESULTS

Typical recordings of the vagal stimulation command, HR, and AP obtained under control and ANG II conditions are shown in Fig. 1*A*. The random vagal stimulation began at 60 s. The HR decreased in response to the random vagal stimulation. ANG II, which did not affect the prestimulation baseline HR, attenuated the magnitude of the vagal stimulation-induced variations in HR. ANG II increased the AP both before and during the vagal stimulation. ANG II did not change the prestimulation or poststimulation CSNA (Fig. 1*B*).

As shown in Table 1, ANG II did not affect the mean HR before stimulation of the vagal nerve, whereas it significantly increased the mean HR during the vagal stimulation period. ANG II attenuated the reduction in HR, which was calculated as the difference between the prestimulation HR and the mean HR observed during the vagal stimulation period. ANG II significantly increased the mean AP both before and during the vagal stimulation period. ANG II did not affect the mean level of pre- or poststimulation CSNA significantly.

Figure 2*A* illustrates the averaged transfer functions from vagal stimulation to HR obtained under the control and ANG II conditions. In the gain plots, the transfer gain was relatively constant for frequencies below 0.1 Hz and decreased as the frequency increased above 0.1 Hz. ANG II decreased the transfer gain for all of the investigated frequencies, resulting in

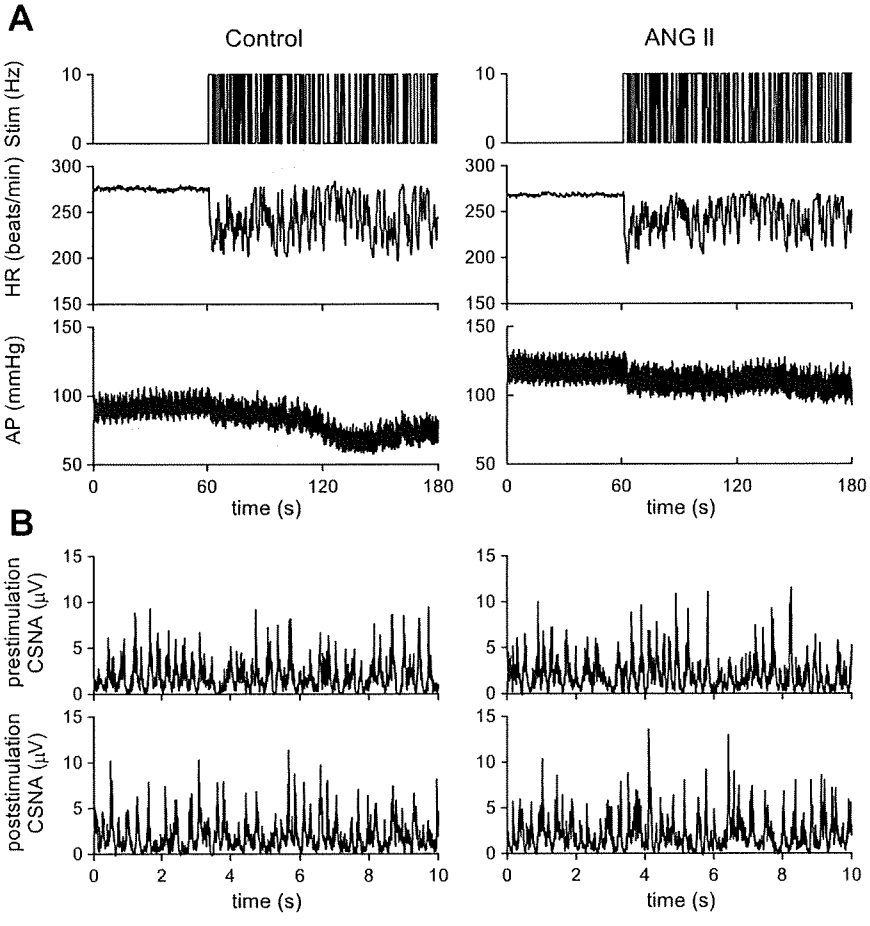

Fig. 1. *A*: representative recordings of vagal nerve stimulation (Stim), the heart rate (HR), and arterial pressure (AP). The *left* and *right* panels show recordings obtained before and during intravenous administration of angiotensin II (ANG II; 10 $\mu g \cdot kg^{-1} \cdot h^{-1}$), respectively. The amplitude of the HR variation in response to vagal stimulation was smaller in the presence of ANG II compared with results obtained without ANG II. *B*: representative recordings of cardiac sympathetic nerve activity (CSNA) under prestimulation baseline and poststimulation conditions. ANG II did not affect the CSNA significantly.

Table 1. *Mean values for HR, AP, and CSNA obtained using the vagal stimulation protocol*

	Control	ANG II	*P* Value
HR, beats/min			
Prestimulation	278±21	281±31	0.60
During stimulation	232±19	245±26*	0.046
Difference‡	−46±6	−37±10†	0.0017
AP, mmHg			
Prestimulation	91±23	127±17†	0.0057
During stimulation	85±24	118±19†	0.0055
Difference‡	−6.3±9.2	−9.2±8.6	0.34
CSNA, μV			
Prestimulation	1.21±0.38 (100%)	1.19±0.46 (98±15%)	0.82
Poststimulation	1.27±0.42 (105±8%)	1.20±0.55 (98±27%)	0.59

Data are means ± SD values; $n = 7$. HR, heart rate; AP, arterial pressure; CSNA, cardiac sympathetic nerve activity. ‡The difference was calculated by subtracting the prestimulation value from the value obtained during the vagal stimulation period in each animal. *$P < 0.05$ and †$P < 0.01$ based on a paired *t*-test. Exact *P* values are also shown.

a parallel downward shift in the gain plot. In the phase plots, the phase approached $-\pi$ radians at 0.01 Hz and the lag became larger as the frequency increased. ANG II did not alter the phase characteristics significantly. In the coherence plots, the coherence value was close to unity in the frequency range from 0.01 to 0.8 Hz. The sharp variation around 0.6 Hz corresponds to the frequency of the artificial ventilation. Figure 2*B* depicts the HR step responses calculated from the corresponding transfer functions. ANG II significantly attenuated the steady-state response without affecting the response speed.

As shown in Table 2, ANG II significantly attenuated the dynamic gain of the vagal transfer function to 76.1 ± 8.5% of the control value without affecting the corner frequency or pure delay. The goodness of fit to the first-order low-pass filter did not differ between the control and ANG II conditions. In the HR step response, ANG II significantly attenuated the steady-state response without affecting the 80% fall time.

Typical recordings of the sympathetic stimulation command, HR, and AP obtained under control and ANG II conditions are shown in Fig. 3*A*. The random sympathetic stimulation began at 60 s. HR increased in response to random sympathetic stimulation. ANG II did not affect the prestimulation baseline HR. The magnitude of the HR variation in response to sympathetic stimulation did not change significantly. ANG II increased the AP both before and during the sympathetic stimulation. ANG II did not change the pre- or poststimulation CSNA significantly (Fig. 3*B*).

As shown in Table 3, ANG II did not affect the mean HR before or during the period of sympathetic stimulation. ANG II did not affect the increase in HR, calculated as the difference between the prestimulation HR and the mean HR in response to sympathetic stimulation. ANG II significantly increased the mean AP both before and during the sympathetic stimulation period. ANG II did not affect the mean level of pre- or poststimulation CSNA significantly.

Figure 4*A* illustrates the averaged transfer functions from sympathetic stimulation to HR obtained under control and ANG II conditions. In the gain plots, the transfer gain decreased as the frequency increased. ANG II did not change the transfer gain markedly. In the phase plots, the phase approached zero radians at 0.01 Hz and increasingly lagged as the frequency increased. ANG II did not affect the phase characteristics significantly. The coherence value was above 0.9 for the frequency range below 0.1 Hz and decreased in the frequency range above 0.1 Hz. Figure 4*B* depicts the HR step responses calculated from the corresponding transfer functions. ANG II did not affect the steady-state response or the response speed.

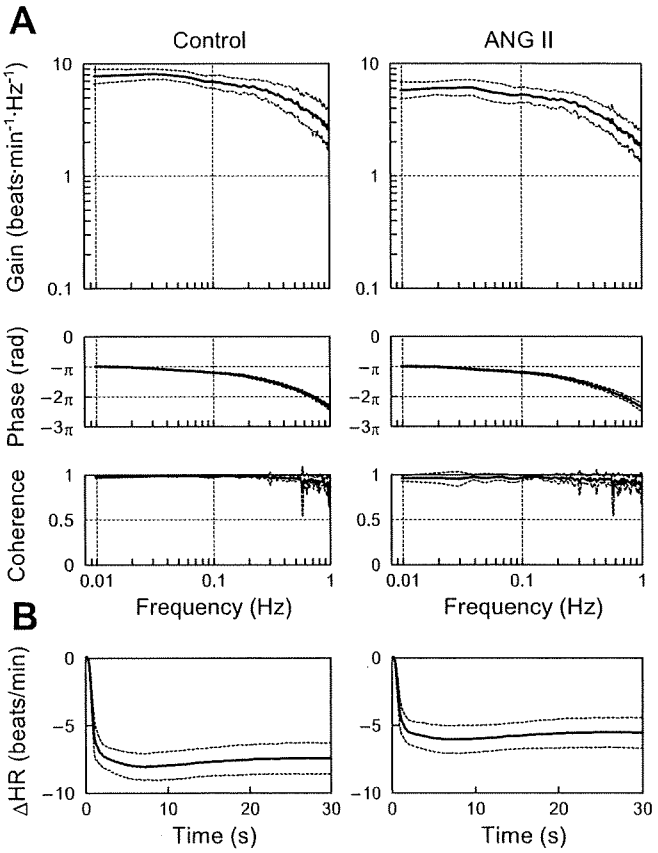

Fig. 2. *A*: averaged transfer functions from vagal nerve stimulation to the HR response obtained before and during intravenous administration of ANG II. Gain plots (*top*), phase plots (*middle*), and coherence plots (*bottom*) are shown. ANG II caused a parallel downward shift in the gain plot. ANG II did not affect the phase plot or coherence plot significantly. *B*: step responses of the HR to a unit change in the vagal stimulation calculated from the corresponding transfer functions. ANG II significantly attenuated the step response of the HR. ΔHR, changes in heart rate. Solid lines indicate mean, and dashed lines indicate mean ± SD.

Table 2. *Effects of ANG II on the parameters of the transfer function and the step response relating to the dynamic vagal control of HR*

	Control	ANG II	*P* Value
Dynamic gain, beats·min^{-1}·Hz^{-1}	7.6±0.9	5.8±0.9*	0.00042
Corner frequency, Hz	0.39±0.12	0.36±0.10	0.12
Pure delay, s	0.48±0.04	0.47±0.06	0.82
Goodness of fit, %	98.8±0.4	98.6±0.8	0.63
Steady-state response, beats/min	−7.4±1.1	−5.6±1.1*	0.0011
80% Fall time	1.31±0.31	1.33±0.37	0.60

Data are means ± SD values; $n = 7$. *$P < 0.01$ based on a paired *t*-test. Exact *P* values are also shown.

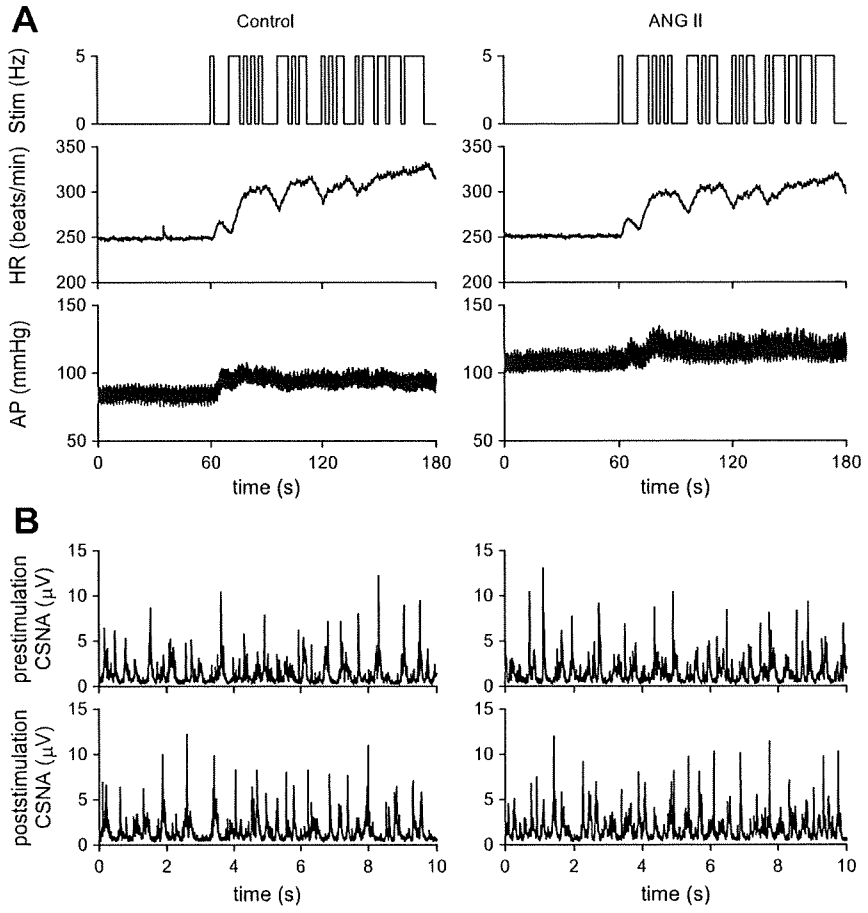

Fig. 3. *A*: representative recordings of cardiac sympathetic nerve stimulation (Stim), HR, and AP. The *left* and *right* panels show the recordings before and during intravenous administration of ANG II (10 $\mu g \cdot kg^{-1} \cdot h^{-1}$), respectively. The amplitude of the HR variation during sympathetic stimulation was unchanged by the addition of ANG II. *B*: representative recordings of CSNA under prestimulation baseline and poststimulation conditions. ANG II did not affect the CSNA significantly.

As shown in Table 4, ANG II slightly attenuated the dynamic gain of the sympathetic transfer function to 92.5 ± 8.9% of the value observed under control conditions. ANG II did not affect the natural frequency, damping ratio, or pure delay. The goodness of fit to the second-order low-pass filter did not differ between the control and ANG II conditions. In the HR step response, ANG II did not affect the steady-state response or the 80% rise time. As shown in Table 5, there were no significant differences in the parameters of the sympathetic transfer function between repeated estimations with an intervening interval of more than 20 min.

Table 3. *Mean values for HR, AP, and CSNA obtained using the sympathetic stimulation protocol*

	Control	ANG II	*P* Value
HR, beats/min			
Prestimulation	267±16	261±19	0.21
During stimulation	317±26	311±23	0.063
Difference†	50±21	50±21	0.94
AP, mmHg			
Prestimulation	74±6	106±15*	0.0011
During stimulation	78±6	110±17*	0.0023
Difference†	4.7±3.6	4.1±5.4	0.71
CSNA, μV			
Prestimulation	0.91±0.71 (100%)	0.98±0.78 (99±19%)	0.22
Poststimulation	0.93±0.72 (101±4%)	1.02±0.81 (104±21%)	0.18

Data are means ± SD values; $n = 7$ except for CSNA data where $n = 5$. †The difference was calculated by subtracting the prestimulation value from the value obtained during the sympathetic stimulation period in each animal. *$P < 0.01$ based on a paired *t*-test. Exact *P* values are also shown.

DISCUSSION

Intravenous administration of ANG II at 10 $\mu g \cdot kg^{-1} \cdot h^{-1}$ increased AP but did not affect mean HR or mean CSNA during prestimulation baseline conditions (Tables 1 and 3), suggesting that ANG II at this dose did not affect the residual sympathetic tone to the heart significantly. ANG II significantly attenuated the dynamic gain of the transfer function from vagal stimulation to HR, whereas it only slightly attenuated that of the transfer function from sympathetic stimulation to HR (Tables 2 and 4).

Effects of ANG II on the transfer function from vagal stimulation to HR. ANG II attenuated the dynamic gain of the transfer function from vagal stimulation to HR without affecting the corner frequency or pure delay (Fig. 2 and Table 2). Several interventions can affect the dynamic gain of the vagal transfer function and significantly change the corner frequency. For example, inhibition of cholinesterase, which interferes with the rapid hydrolysis of ACh, augments the dynamic gain and decreases the corner frequency (29). Moreover, blockade of muscarinic K^+ channels, which interferes with fast, membrane-delimited signal transduction, has been shown to attenuate the dynamic gain and decrease the corner frequency (26).